Russian Chemical Reviews **80** (12) 1159 – 1177 (2011) © 2011 Russian Academy of Sciences and Turpion Ltd

DOI 10.1070/RC2011v080n12ABEH004239

Structural and chemical aspects of the design of multiferroic materials

A R Akbashev, A R Kaul

Contents

I.	Introduction	1159
II.	General information on the multiferroics	1159
III.	Homogeneous multiferroics	1160
IV.	Composite multiferroics	1170
V.	Conclusion	1171
VI.	Appendix	1172

Abstract. The existing approaches to the chemical design of multiferroic materials are described in detail. The structural and functional features of the known homogeneous multiferroics and the latest advances in the field of multiferroics are considered. The features of synthesis of composite magnetoelectrics with specified properties are considered separately. The special emphasis is made on epitaxial stabilization as a key method for the production of new magnetoelectric materials and controlled change of their physical properties. The bibliography includes 218 references.

I. Introduction

During the past 10 years multiferroics have become a popular object of the investigation in chemistry and solid-state physics. According to the definition given by Schmid,[1] multiferroics are compounds comprising at least two of the three types of ferro-ordering: electrical, magnetic and mechanical.† Strictly speaking, some other classes of compounds (for example piezoelectrics and piezomagnetics) also fall under this definition, so the trend has appeared to use the term multiferroics for the compounds with both ferroelectric and (anti)ferromagnetic type of ordering. In the present review, we shall interchange the terms 'multiferroics' and 'magnetoelectrics' but we also want to underline that strictly speaking, this is not correct, as crystals are considered as magnetoelectric when they exhibit magnetoelectric effect, and this is not necessarily connected with the presence of, for example, electric polarization, which should be present in multiferroics by definition.[2] Earlier it was considered that there are practically no compounds with simultaneous ferroelectric and magnetic types of ordering. This was due both to the lack of physical and structural investigations of the new materials and to the absence of some modern methods of their synthesis. The today interest in the multiferroics emerged after the appearance of the other, new and related areas in physics and solid state chemistry connected with the high-temperature superconductivity, strong electron correlations, charge and spin frustrations in crystals.

The interplay of the ferroelectric and magnetic subsystems is characterized by the magnetoelectric effect, which was originally found in the magnetoelectric Cr_2O_3;[3] however, until recently magnetoelectrics have not been actually investigated as potential materials for technological applications due to low of magnetoelectric response. The modern electronics, which broadly applies the nanotechnological approaches and solutions, shows its main interest in nanomaterials and thin films with the magnetoelectric properties. On the other hand, it should be noted that significant success in the preparation of the new and promising multiferroics is mainly connected with the appearance and wide popularity of different methods for the preparation of thin epitaxial films. New crystal structures have been stabilized and original composite materials with the magnetoelectric properties have been obtained with the use of the epitaxy, while ferroelectricity has been induced by crystal lattice strains in known magnetic compounds.

II. General information on the multiferroics

An early work dedicated to the multiferroics was carried out by Astrov,[3] who proved experimentally the presence of the magnetoelectric effect in the chromium(III) oxide and investigated this effect. Since that, a big number of single-phase multiferroics have been discovered, including $BiFeO_3$,

† The ferrotoroid ordering is not considered in this review.

A R Akbashev, A R Kaul Department of Materials Science and Department of Chemistry, M V Lomonosov Moscow State University, Leninskie Gory 1, 119991 Moscow, Russian Federation. Fax (7-495) 932 88 46, tel. (7-495) 939 14 92, e-mail: andrew.akbashev@gmail.com (A R Akbashev), kaul@inorg.chem.msu.ru (A R Kaul)

Received 22 June 2011
Uspekhi Khimii **80** (12) 1211 – 1230 (2011); translated by Z P Svitanko

$HoMnO_3$, $TbMn_2O_5$, $DyMnO_3$, $LuFe_2O_4$, $Ni_3V_2O_8$, $MnWO_4$, *etc*. (see Appendix). In the majority of cases, these compounds are oxides but halogen-containing compounds, phosphates and chalcogenides are also known. At present, the search for the new multiferroics is being carried out not only among inorganic but also among organic [4] and organometallic [5,6] compounds. The development of the theory of the magnetoelectricity allowed understanding and in many cases successful prediction of the magnetic and ferroelectric properties of single-phase multiferroics, which significantly facilitates the search for the new magneto-electrical materials.

A peculiarity of the multiferroics is the possibility of the co-existence of two types of ferro-ordering (magnetic and electric), which has been considered earlier only hypothetically. The main reason for this was the common opinion about the covalent character of the origin of ferroelectricity, perovskite ($BaTiO_3$) being usually provided as an example. The polarization in $BaTiO_3$ appears due to the absence of electrons in the outer d-shell of the Ti^{4+} ions and the subsequent hybridization with the outer p-shells of the oxygen atoms. However, unpaired electrons in the d-shells are required for the appearance of the exchange interaction and subsequent magnetic ordering in the transition metal compounds, which in turn significantly suppresses the tendency for the appearance of the dipole moment upon the hybridization. Other mechanisms of the polarization appearance in crystals have become known owing to the results of the intensive investigations and are often used as a basis for the classification of the multiferroics. The ferroelectrics are classified into proper and improper ones depending on the difficulty of the distortion of the initially symmetrical crystal structure.[7] In the former case, a conventional phase transition into the polar state of the crystal occurs either due to a small displacement of the ions with the formation of partially covalent bonds (exemplified by $BaTiO_3$) [8] or upon the loss of centrosymmetric position of the $6s^2$ electron pair (exemplified by $BiFeO_3$).[9] In the case of improper ferroelectricity, the phase transition is a result of some more complicated lattice distortions and the spontaneous polarization is exhibited as a secondary effect. Usually, the improper ferroelectricity is caused by the specific magnetic ordering (magnetic ferroelectricity, as in $TbMnO_3$, $DyMnO_3$),[10,11] spontaneous lattice distortion (geometrical ferroelectricity, as in $HoMnO_3$) [12] or electron correlations [electronic ferroelectricity, as in Fe_3O_4,[13] $LuFe_2O_4$ (Ref. 14)].

Thus, the magnetically dependent and magnetically independent types of electric ordering are distinguished in multiferroics. In the first case, the polarization directly results from the presence of a certain spin structure, while in the second case, the magnetic sublattice exists independently of the ferroelectric ordering.

In the present review, we consider mainly the single-phase (or homogeneous) multiferroics, the peculiarities of their crystal chemistry and synthesis. The consideration is based on the classification in terms of the composition and crystal structure type of the compounds and the arising ferroelectric ordering and its connection to the magnetic subsystem. Among the chemical approaches used to alter the functional properties of the multiferroics, special attention is paid to the chemical doping and preparation of thin epitaxial films. In the last part of the review, the chemical principles of the preparation of the composite magnetoelectric materials as thin films and in the bulk state are briefly surveyed.

III. Homogeneous multiferroics

1. Bismuth ferrite

Perovskite and perovskite-like structures have become the basis for the creation of numerous functional materials due to the simplicity of their crystal structure and a large variety of compositions. Bismuth ferrite ($BiFeO_3$) was one of the first investigated multiferroics with the perovskite structure. It was also found that it possesses record-breaking ferroelectric (T_C = 1103 K) and antiferromagnetic (T_N = 643 K) ordering temperatures (T_C is the Curie temperature, T_N is the Néel temperature), but the maximum value of the polarization (P) in the single-crystal $BiFeO_3$ turned out to be very small ($3-6$ μC cm^{-2}).[15] In contrast to the single crystals, the measurements of the pyroelectric current in the thin epitaxial films of bismuth ferrite‡ have shown high polarizability, which reached values of $60-100$ μC cm^{-2} (Ref. 16). It is considered that the main reason for such small polarization in the previously investigated bulk crystals is the leakage current caused by nonstoichiometry and defects, which was eliminated only in the thin film state and later in the high-quality single- and polycrystals.[17–19] The synthesis of the $BiFeO_3$ phase is complicated, on one hand, by high probability of the formation of impurity phases such as sillenite $Bi_{25}Fe_xO_{20\pm\delta}$ (isostructural to the metastable γ-Bi_2O_3) and $Bi_2Fe_4O_9$ at the grain boundaries of polycrystalline ceramics and, on the other hand, by the strong dependence of the physical properties on the oxygen stoichiometry and crystal perfection. Both low leakage currents and the presence of magnetic moment in the crystal are required for the practical application of bismuth ferrite; hence, special attention has been paid to the improvement of the ferroelectric characteristics and the destruction of the cycloidal antiferromagnetic order in $BiFeO_3$. The local spin structure in bismuth ferrite is of the G type (every Fe^{3+} ion is surrounded by six Fe^{3+} ions with the opposite spins), but the Dzyaloshinskii–Moriya interaction disrupts the antiparallel orientation of the spins ('skews' the antiparallel spins), which form the incommensurate spin cycloid. Different ways of the cycloid degradation are considered below.

a. Dependence of the properties of $BiFeO_3$ thin films on their structure and strained state

Thin films of $BiFeO_3$ of different symmetry can be obtained using the epitaxy effect and single-crystalline substrates with different surface orientation. So, the monoclinic phase is crystallized on the (001) and (101)$SrTiO_3$ substrates, while the rhombohedral phase is preserved on (111)$SrTiO_3$.[20,21] One of the most significant results obtained by the authors of this review is the discovery of noticeable sensitivity of the paraelectric–ferroelectric transition temperature to the epitaxial strain in the films. The Curie temperature is 650 °C in the case of films that experience strong epitaxial strain, which is almost 100 degrees lower that the analogous value for the weakly strained films ($T_C \approx 750$ °C). The bulk bismuth ferrite has T_C = 830 °C. The magnetic measurements of the strained

‡ The measurement of the pyroelectric current is a standard method to obtain the values of the polarization change (ΔP) in ferroelectrics.

films obtained by metal-organic chemical vapour deposition (MOCVD) have shown the saturation magnetization value (P_s) to be close to that for films prepared by pulse laser deposition (PLD).[22–24] Apparently, the destruction of the spin cycloid occurs with the formation of the homogenous antiferromagnetic order, the skewed spins in which give rise to a weak magnetic moment of thin film specimens.

The magnetic structure of $BiFeO_3$ represents a spin cycloid with the modulation of 62 nm. The nanodomain nature of films possessing the so-called variant structure[25] can induce partial destruction of such magnetic structure when the sizes of the epitaxial domains are smaller than or incommensurate with the modulation length. Indeed, the formation of the variant structures has been observed during the preparation of the $BiFeO_3$ films by MOCVD[25] on cubic (001)$ZrO_2(Y_2O_3)$.[26] The typical size of the variant domains was about 20–40 nm; however it reached 200 nm in some cases (apparently due to the high lateral diffusion of the film components). The saturation magnetization of the films with the variant structure (at 5 K) was fourfold higher than the magnetic moment of the strained $BiFeO_3$ films, and as compared with relaxed films the magnetization has increased 20-fold. This points to the high efficiency of the used method for the preparation of the variant structure of films upon the change of the magnetic properties of the spin-modulated magnets.

b. Influence of the cation doping on the $BiFeO_3$ properties

The bismuth ion in $BiFeO_3$ has been mainly replaced by alkaline earth metal ions, lanthanides, Pb, and K, while iron was replaced by Co, Mn, Mo, Nb, Ni, Sc, Ti, V and Zr. In particular, for the solid solutions (Bi,R)FeO_3 (R = Dy, Tb, Eu, Gd), invariability or decrease in the leakage current was observed in the majority of the investigations along with the significant increase in the magnetic moment (usually due to the crystal structure distortion) both for the epitaxial and polycrystalline films.[27–30]

The investigations have shown[31] that the introduction of foreign oxides into the $Bi_2O_3-Fe_2O_3$ system favours separation of the $BiFeO_3$ phase into phases with the sillenite structure with a high Bi^{3+} content and Bi-deficient phases based on $Bi_2Fe_4O_9$. Moreover, a big number of the individual $Bi_{12}M_xO_{20\pm\delta}$ phases that crystallize in the sillenite structural type are known,[32] as well as innumerable number of solid solutions based on them, which significantly complicates the preparation of the $BiFeO_3$ homogeneous phase.

2. Solid solutions with the perovskite structure

The first attempts to synthesize a single-phase multiferroic were performed by the group of Smolenskiy[33,34] in 1961. The main idea was doping of the octahedral positions in ferroelectrics with the perovskite structure [for example $Pb(Zr,Ti)O_3$] by magnetic ions (for example Fe^{3+}, Mn^{3+}, Co^{2+}). Thus, the compound $Pb(Fe_{2/3}W_{1/3})O_3$, which is a ferroelectric (T_C = 180 K) and an antiferromagnet (T_N = 370 K), has been synthesized.[33] Later, a big variety of solid solutions that combine ferroelectrically active and magnetic ions have been prepared.[35] Currently this issue receives particular attention due to the unique properties of such single-phase materials.[36] Besides the relatively high temperatures of the ferroelectric and magnetic orderings, mixed multiferroics often show electronic phase separation into magnetic and ferroelectric nanoregions due to the problem mentioned above (see Section II) concerning the requirement of simultaneous presence and absence of electrons in the d-level of the transition metals for the two types of ordering.[37–41] The mesoscopic model describing the behaviour of such multiferroic relaxors was reported.[41]

3. Boracites

The boracites $M_3B_7O_{13}X$ (M = Mn, Fe, Co, Ni; X = F, Cl, Br, I) are also among the first discovered magnetoelectrics. The paraelectric phase of the boracite has a cubic structure (space group $F43c$) in which M and X atoms form chains along crystallographic axes that intersect in the halogen atom positions and are located in the framework of BO_4 tetrahedra and OBO_3 pyramids (in the OBO_3 pyramids one of the B–O bonds is ~0.2 Å longer than the other) (Fig. 1).[42] The boracite $Ni_3B_7O_{13}I$ is a piezoelectric – antiferromagnet below 120 K, while below 64 K it is a ferroelectric – ferromagnet with polarization direction being dependent on the magnetization vector.[43] Boracites are prepared most often by the chemical vapour transport method.[44] In this process, the crystals grow from the heated vapour phase that contains the halide MX_2 and B_2O_3. Later, a simpler approach to the synthesis has been suggested,[45] which consists of autoclaving of a mixture of $MX_2 \cdot n\,H_2O$ with H_3BO_3 at 240–270 °C with subsequent washing out of the remaining boric acid with water.

4. Orthophosphates

The orthophosphates $LiMPO_4$ (M = Fe, Co, Ni, Mn) have the olivine structure built of MO_6 octahedra which are linked into layers and share oxygen atoms with the PO_4 tetrahedra, which also form layers (see Fig. 1). The lithium ions are located in between the layers, which provides high diffusion mobility. The mixed valence of the transition metals in these compounds determines the mechanism of charge compensation upon the variation of the lithium contents. Due to these peculiarities, the $LiMPO_4$ orthophosphates, especially $LiFePO_4$ started to be used in the last years as effective cathode materials for lithium batteries, a substantial body of literature has evolved on this topic.[46–48] In the context of the present review, it is important that orthophosphates are also antiferromagnets with the Néel temperature of 20–40 K. Despite the strong superexchange interaction in the layers of the condensed MO_6 octahedra, weak exchange along the M–O–P–O–M bonds is also realized between them, which makes significant contribution to the formation of the three-dimensional antiferromagnetic ordering.[49] This is most pronounced for $LiNiPO_4$, while for $LiMnPO_4$, for example, the exchange between the MnO layers is too weak for the formation of the incommensurate spin system.[50] However, in $LiNiPO_4$ the application of a $B < 12$ T magnetic field induces the ferroelectric ordering where the commensurate spin structure does not turn into the incommensurate one, and in the $B > 12$ T field, the spin structure in the orthophosphate $LiNiPO_4$ becomes incommensurate and the polarization vanishes.[51]

5. Multiferroics on the basis of the strained epitaxial cubic structures

The search for the ferroelectric properties in insulators by distorting or mechanically stressing their crystal structures has become very popular recently. Such stresses appear naturally in the heteroepitaxial thin films due to the difference between the unit cell parameters and the thermal expansion coefficients of the film material and the single-

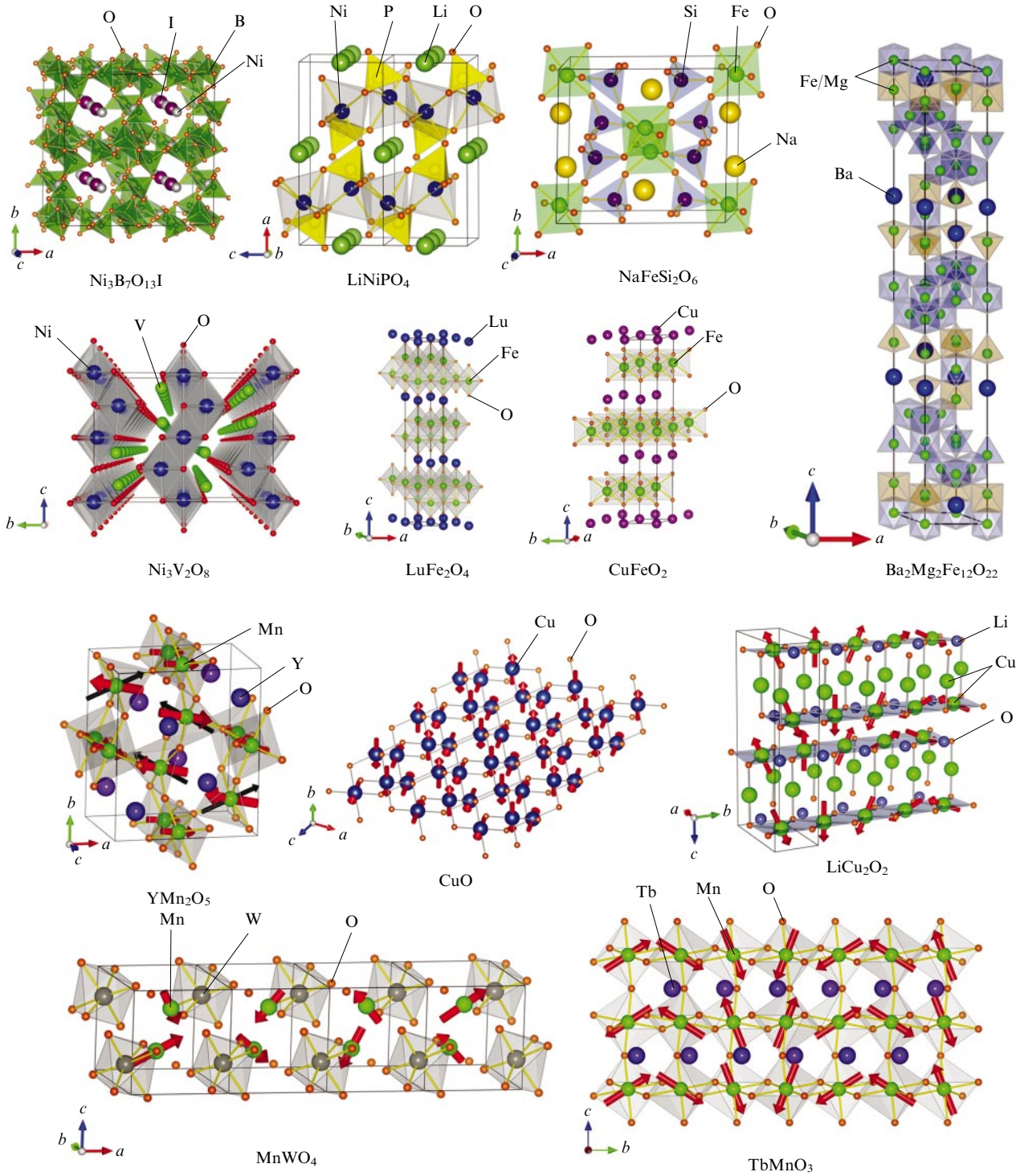


Figure 1. Crystal structures of the inorganic multiferroics. For some compounds, the directions of spins are shown with red arrows, the dipole moments are indicated by black arrows.

crystalline substrate material. One of the most well-known examples is strontium titanate ($SrTiO_3$), which exhibits paraelectric properties in the bulk state all the way down to 0 K (the so-called quantum paraelectricity, which manifests itself in the absence of the ferroelectric order due to the quantum fluctuations, *i.e.*, zero-point vibrations of atoms), but which can easily be transformed into the ferroelectric state upon weak external impact on the crystal lattice (mechanical strain, chemical doping). The appearance of the polarization upon application of the mechanical strain or doping is quite possible in the quantum paraelectrics, which is connected with the high instability of the quantum

paraelectric state and the ease of its destruction. Thus, T_C for the ferroelectric–paraelectric transition in the strained epitaxial $SrTiO_3$ films may reach room temperatures.[52] Similar effect in $KTaO_3$ films leads to an even more stable ferroelectric state with $T_C \approx 700$ K.[53]

Another example is the perovskite $EuTiO_3$, which is a quantum paraelectric in the bulk state (similar to $SrTiO_3$) and an antiferromagnet (AFM/PE). The biaxial strain emerge in the thin films of $EuTiO_3$ obtained using molecular-beam epitaxy on the (001)$DyScO_3$ substrate;[54] when the strain exceeds (ε) $\sim$1%, the transition to the ferroelectric ferromagnetic phase (FE/FM) occurs.§ Near the transition point ($\varepsilon \approx 1\%$), strong binding of the IR-active phonon with the magnetic and elastic subsystems leads to an easy reversible AFM/PE $\rightarrow$ FE/FM transition induced by application of the external magnetic/electric field.[54, 55] The magnetoelectric effect connected with such phase control (magnetic and electric) possesses certain specific features. In particular, using the external field, one can switch on the magnetization or polarization, while the control of the ordering vector or switching between the opposite directions of the polarization/magnetization is actually impossible.[55]

The antiferromagnetic paraelectric $SrMnO_3$ with strong spin–phonon interactions is another compound for which the multiferroic properties in thin films are only predicted theoretically.[56] The transition into the ferroelectric–ferromagnetic state with high ordering temperatures is expected for thin films of this compound even at the strain of $|\varepsilon| > 3\%-4\%$, while for the boundary strain values, strong magnetolectric effect is likely to arise between the initial antiferromagnetic and mechanically induced ferromagnetic phases, similar to that confirmed for $EuTiO_3$.

Calculations show[57] that biaxial strains should lead to the polarization of the thin films even for such oxides as BaO, SrO and CaO, which crystallize in the NaCl structural type. This unexpected effect is caused, apparently, by the hybridization of the metal d-orbitals and oxygen 2p-orbitals in the alkaline earth metal oxides,[58] which are highly sensitive to the variation of the interatomic distances. The authors have proven that upon the achievement of the critical biaxial strain the alkaline earth metal oxides pass into the ferroelectric state; however, the paraelectric state with a strong dependence of the lateral optical phonon frequency and the dielectric constant on the strain should be observed at the strain values lower than the critical ones.

The semiconductor EuO possessing a similar cubic structure (NaCl type) is interesting from the point of view of potential magnetoelectric properties. Under the biaxial strains of > 4% (both shrinking and stretching ones), the appearance of polarization[57] and increase in T_C of the ferromagnetic ordering have been predicted for it.[59] However, despite the fact that the strained thin films of EuO have been prepared,[60] the investigation of their magnetic and ferroelectric properties has not been carried out to a full extent, since the work with EuO is hampered by the fact that this phase is stable only at an extremely low partial oxygen pressure.

§ ε is the parameter that characterizes the difference between the unit cell parameters of the film and the substrate material.

6. Hexagonal and perovskite manganites of lanthanides

The lanthanide manganites $RMnO_3$ typically having orthogonally distorted perovskite structures or hexagonal structures (crystallization of $RMnO_3$ in either of them is determined by the ion radius of the trivalent lanthanide) stand out from the widely investigated multiferroics. The $RMnO_3$ perovskite structure remains stable under normal conditions in the range of the ionic radii $r_{Dy} \leqslant r_R \leqslant r_{La}$,[61] but under high pressure the perovskite phase can be stabilized also for the other members of the series. The hexagonal structure of the $LuMnO_3$ type (space group $P6_3cm$) becomes stable with the decrease in the ionic radius R^{3+} in the series Y, Ho, Er, Tm, Yb, Lu; this structure can be described as the close sphere packing of the oxygen ions (ABCACB) in which the Mn^{3+} ions have the coordination number (CN) of 5 (trigonal bipyramid), while R^{3+} ions are located in single-capped seven-vertex octahedra (CN = 7).[61, 62] The hexagonal manganites $RMnO_3$ are geometrical ferroelectrics, *i.e.*, the ferroelectric ordering in them ($T_C \approx 900$ K) is due only to the structural distortions: the cooperative distortion of the bipyramids below the Curie temperature shifts R^{3+} ions along the *c* axis, giving rise to ferroelectricity.[63] The inclination angle of the MnO_5 polyhedra increases with the decrease in the ionic radius R^{3+} in such a way that the ferroelectric polarization attains its maximum for Sc^{3+} (Ref. 64). The two-dimensional antiferromagnetic ordering of the Mn^{3+} ions in the *ab* plane with $T_N \approx 100$ K is observed for the hexagonal manganites. It was established[65] that the heteroepitaxy on appropriate substrates allows for a significant widening of the limits of the geometrical tolerance for the $RMnO_3$ structure and for obtaining the hexagonal modification of $RMnO_3$ also for ions larger than Ho (namely, Dy, Gd, Eu). According to the theoretical model of the epitaxial stabilization, the critical thickness of the stabilized hexagonal layer decreases along with the increase in the instability of the hexagonal phases in the bulk state, *i.e.*, with the increase in the lanthanide ionic radius.[66] The stabilization of the hexagonal lanthanide manganites is possible on the cubic substrate structures with the (111) cut plane, for example (111)$ZrO_2(Y_2O_3)$[65] or (111)MgO (Fig. 2 *a*),[65, 67] and also on hexagonal substrates in the (0001) orientation, such as ZnO, GaN and hexagonal $YMnO_3$.[68–70] For the epitaxially-stabilized manganites $RMnO_3$ (R = Eu–Dy), the magnetic and ferroelectric properties are poorly studied, but the available data point to the presence of magnetoelectric properties. Thus, for $RMnO_3$ (R = Dy, Tb, Gd) the magnetic ordering is observed below 60–70 K[71–74] along with the electrical polarization. An outstanding result is the discovery of the possibility for the control of the magnetic phase by the applied electric field in $HoMnO_3$.[75] The AFM-sublattice of the Ho^{3+} ions in the electric field becomes ferromagnetic bellow the Néel temperature of the Mn^{3+} ions ordering (75 K). This is due to the strong magnetoelectric effect caused by the influence of the ferroelectric ordering on the interactions between the magnetic Ho^{3+} and Mn^{3+} ions.

Among $RMnO_3$ manganites with the perovskite structure, $TbMnO_3$, $DyMnO_3$, (Eu,Y)MnO_3, $YMnO_3$, $HoMnO_3$ and $TmMnO_3$ are multiferroics.[76] The distortions of the perovskite cubic structures dependent on the effective size of cations in the R-sub-lattice are typical of all lanthanide manganites. These distortions, which can be described as a result of the correlated rotation of the MnO_6 octahedra,[76]

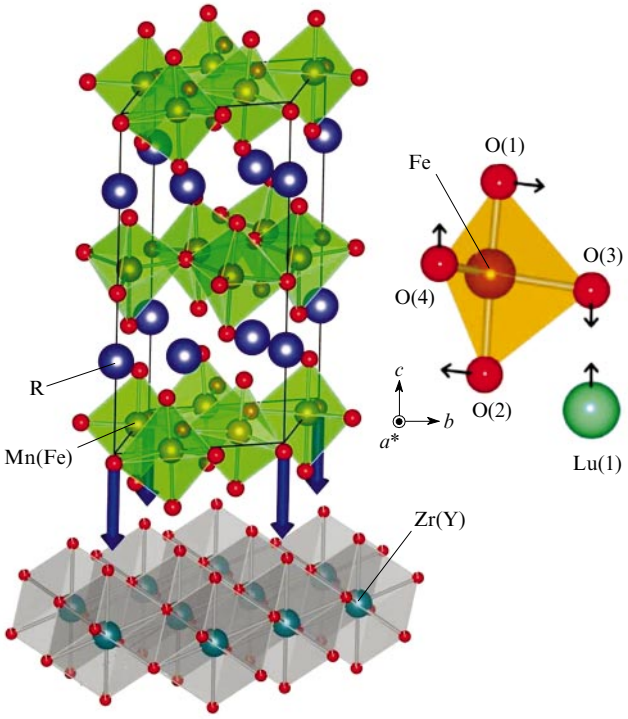


Figure 2. Epitaxial stabilization of the hexagonal $RMnO_3$ and $RFeO_3$ (R is lanthanide) on the $(111)ZrO_2(Y_2O_3)$ substrate (*a*) and the relative positions of the FeO_5 trigonal bipyramid and Lu(1) (*b*) [the arrows denote the directions of the atom displacements due to the hybridization of the atomic orbitals of Lu(1) and O(3)].[85]

are directly linked with the magnetic structure of the manganites in the ground state: for the least distorted structures (R = La – Eu), the antiferromagnetic ordering of the A-type is observed, which is replaced by the E-type ordering for the compounds with the most distorted perovskite structure (R = Ho – Lu). The distortion of the perovskite lattice in the manganites formed by the intermediate lanthanides (R = Gd, Tb, Dy, $Eu_{1-x}Y_x$) leads to the intermediate magnetic ordering characterized by the strong spin frustrations. Thus, $TbMnO_3$ at $T < 41$ K possesses an incommensurate sinusoidal spin structure, its symmetry does not allow the polarization to appear; however, bellow 28 K it turns into the cycloid spin function with the concomitant emergence of the polarization.[77,78] In the case of $GdMnO_3$, the polarization emerges only in the applied magnetic field, which is apparently due to the transformation of the spin structure from the canted antiferromagnetic to the cycloid one.[76] Due to the discovery of the strong magnetoelectric effect in $RMnO_3$ (R = Tb, Dy), the metastable manganites with the perovskite structure $RMnO_3$ (R = Ho – Lu, Y) have been investigated both theoretically and experimentally.[77,78] Similarly to the hexagonal $RMnO_3$, the perovskite modification can be epitaxially stabilized on appropriate substrates such as $LaAlO_3$ and $SrTiO_3$.[79] As for the stabilized perovskites, the electric polarization has been discovered in the antiferromagnets $YMnO_3$,[80] $HoMnO_3$,[80] $TmMnO_3$.[81]

It is known that the orthoferrites $RFeO_3$ formed by all lanthanides (R = La – Lu) have perovskite structure, under normal conditions, in which the Fe^{3+} ions are in the octahedral environment. However, there are very scarce data in the literature on hexagonal lanthanide ferrites, direct structural analogues of the hexagonal manganites discussed above. The hexagonal modifications of $RFeO_3$ (R = Y, Eu, Yb) were prepared for the first time as nanoparticles, which were stabilized, apparently, due to the significant input of the surface free energy.[82] It turned out that the crystal structures of the nanoparticles of the hexagonal $EuFeO_3$ and $YbFeO_3$ significantly differ from the structure of the hexagonal orthoaluminate $YAlO_3$, characterized by the centrosymmetrical space group $P6_3/mmc$, and are identical to the structure of the hexagonal $LuMnO_3$. For the first time,[83] the hexagonal $RFeO_3$ (R = Eu – Lu) phases were successfully stabilized as thin film and it was shown that the trends of their epitaxial growth coincide with those for the hexagonal manganites $RMnO_3$ (see Fig. 2 *a*). At present, there is no data on the physical properties of such hexagonal ferrites but there are grounds to expect them to exhibit multiferroic properties. The authors of this review have shown the presence of a weak ferromagnetic ordering in thin films of the hexagonal $RFeO_3$ (R = Lu, Er, Ho, Dy, Tb) below $T_N = 120 - 140$ K.[84] The hexagonal phase of $LuFeO_3$ is fully isostructural to the ferroelectric phase of $LuMnO_3$ (space group $P6_3cm$),[85] while a significant difference in the lengths of two adjacent bonds Lu(1) – O(3) and Lu(2) – O(4) (0.18 Å) along the crystallographic [001] direction of the $LuFeO_3$ orthoferrite observed also in $LuMnO_3$ suggests the presence of ferroelectricity in the hexagonal lanthanide ferrites (see Fig. 2 *b*). Presumably, the high contribution of hybridization of the atomic orbitals between Lu and O atoms leads to a shorter distance between them and lowers their symmetry $P6_3/mmc \rightarrow P6_3cm$. Similar picture of lowering of symmetry is known, for example, for the hexagonal $YMnO_3$,[86] for which the distortion and rotation of the MnO_5 bipyramids accompanied by the hybridization of the Y and O orbitals also induce ferroelectricity.[87]

7. Multiferroics with charge ordering

Typical representatives of the multiferroics in which polarization is of electronic origin and is connected with the strong correlation effects are ferrites of trivalent metals (lanthanides and indium) described as RFe_2O_4 (R = Lu, Yb, Tm, Y, Er, Ho, In) and corresponding to the intergrowth phases of the $(RMO_3)_n(MO)_m$ type. Among the investigations of RFe_2O_4, noteworthy are the studies of Ikeda and co-workers[14,88] in which the polarization in $LuFe_2O_4$ was found and its electronic nature was established. The ferrite RFe_2O_4 has a rhombohedral structure (space group $R3m$) and consists of Fe_2O_2 and LuO_2 layers alternating along the *c* axis with the disposition of atoms in the vertices of the triangles (see Fig. 1). The Fe^{2+} and Fe^{3+} ions in Fe_2O_2 occupy positions in the trigonal planar structure with equal probabilities; this leads to charge frustrations.[89] The charge ordering appears in the layers below 500 K, while below 330 K it becomes three-dimensional and induces polarization. The magnetic ordering appears below 240 K, and the polarization value increases by $\sim 30\%$;[14] however, there is no established opinion on the type of the magnetic ordering. In particular, the single-crystal neutron diffraction data for $LuFe_2O_4$ have shown the presence of the three-dimensional ferromagnetic structure,[90] but later several transitions to different states of the spin glasses were found (at 225, 170 and 55 K).[91] These differences can be connected either wither with the poorly investigated magnetoelectric interaction in RFe_2O_4, or, what is more probable, with the differences in the oxygen

stoichiometry of the samples, which has a strong influence on the physical properties of RFe_2O_4. It is known, for example, that for $YFe_2O_{4-\delta}$ at $\delta > 0$ the three-dimensional magnetic ordering is observed, while it becomes two-dimensional in the stoichiometric samples.[92] The zone melting method in the atmosphere with controllable partial oxygen pressure [$p(O_2)$], for example, in the $CO-CO_2$ mixtures,[93] is being used for the preparation of the RFe_2O_4 single crystals with the required oxygen stoichiometry, and note that the growth of crystals doped by a divalent metal (for example, Mg or Co) is easier and is carried out in air. The presence of the temperature gradient in the zone melting furnace can be the reason for the deviation of the crystals from the required composition and oxygen stoichiometry.[94] Some decrease in T_C (from 256 to 242 K) was observed in the series $YbFe_2O_4-LuFe_2O_4-InFe_2O_4$; however, with the replacement of a half of Fe^{2+} ions by Cu^{2+}, the Curie temperature has conversely increased from 45 K for $YbFeCuO_4$ up to 70 K for $InFeCuO_4$.[95] It is interesting that in the systems $In_2O_3-M_2O_3-M'O$, the compounds $InGaCoO_4$, $InFeCuO_4$ and $InGaMnO_4$ are isostructural to $YbFe_2O_4$; however, $InFeCoO_4$, $InGaFeO_4$, $InGaNiO_4$ and $InFeMgO_4$ possess the spinel structure, while the solubility of $InGaCoO_4$, which is also isostructural to $YbFe_2O_4$, in the Ga_2CoO_4 spinel reaches 40%.[96] This points to a relatively small difference between the Gibbs energies for the formation of the phases of $YbFe_2O_4$ type and spinel for some compounds in the considered systems. The small energy difference between two polymorphs of identical compositions provides the possibility for the epitaxial stabilization of the phases that have the spinel structure under normal conditions in the $YbFe_2O_4$ type through the variation of the structure and substrate parameters. At present, thin epitaxial films RFe_2O_4 are prepared by direct PLD.[97,98] Such films can be prepared also by chemical precipitation method if the condition of the low partial oxygen pressure is met during the precipitation process or the subsequent calcination. Thus, the authors of the review have tested a two-stage MOCVD synthesis of $LuFe_2O_4$ phase on the cubic $ZrO_2(Y_2O_3)$ substrate comprising deposition of the heterogeneous $LuFeO_3+Fe_2O_3$ film from vapours of dipyvaloylmethanates of the corresponding metals and the subsequent annealing with a getter (gas absorber), which sets the desired $p(O_2)$ value for the reduction of Fe^{3+} to Fe^{2+}. The obtained samples really contained the epitaxial phase of $LuFe_2O_4$ together with complete elimination of the $LuFeO_3$ phase.

Another multiferroic with the polarization caused by charge ordering is the ferrimagnetic magnetite Fe_3O_4, which has an inverse spinel structure. The polarization emerges below the Verwey point (120 K), and there is still no unambiguous opinion about its origin. The most probable one is that it is connected with the bond length variation along with the changing of the valence state of the iron ions in the crystal lattice.[99]

Upon doping of lanthanide manganites by divalent metal ions (Ca^{2+}, Sr^{2+}, Ba^{2+}), Mn^{4+} ions appear in the crystal structure of the perovskite apart from the Mn^{3+} ions, which leads to the possibility of emergence of different types of ordering and spin interactions among which the charge ordering plays the main role. Above the charge ordering temperature (T_{co}), the Mn^{3+} and Mn^{4+} ions are chaotically distributed over the entire crystal and below this temperature they occupy strictly defined positions in the crystal structure. Usually two types of the charge ordering are distinguished: the ordering of the Ziner polarons[100] and the ordering of ion charges. From the chemical point of view, the former case represents the periodical alternation of non-equivalent chemical bonds, while the latter case is the ion charge variation. The spatial inversion breaks and polarization appears when both types of charge orderings exist in the crystal.[101] The appearance of polarization predicted in numerous theoretical papers (see for example Ref. 101) for $Ln_{1-x}M_xMnO_3$ (Ln = La, Pr; M = Ca, Sr) can hardly be verified experimentally, as direct polarization measurement is complicated by the low electric resistance of the obtained samples. The authors who draw conclusions about transition to the ferroelectric phase use indirect reasons,[102,103] and additional investigations are required for the reliable confirmation of the existence of the ferroelectric ordering.

8. Multiferroics with the collinear spin ordering

It turned out that manganites with the general formula RMn_2O_5 have complicated magnetic ordering and ferroelectric properties, which depend on the temperature and the applied magnetic field. These compounds formed by all lanthanides have orthorhombic crystal structure (space group *Pbam*, $Z = 4$).[104,105] Manganese ions occupy two types of crystallographic positions, distorted octahedron $Mn^{4+}O_6$ (CN = 6) and slightly distorted square pyramid $Mn^{3+}O_5$ (CN = 5), in equal quantities. The octahedra form infinite chains along the *c* axis, which are linked by the MnO_5 pyramids and two-cap RO_8 antiprisms (see Fig. 1). The structural peculiarities of the RMn_2O_5 manganites are such that Mn^{3+} pyramids are located around Mn^{4+} ions encapsulated into oxygen octahedra. Due to the strong magnetic frustrations, this leads to the antiparallel ordering of the spins of Mn^{4+} ions with one type of Mn^{3+} ions and canted parallel ordering with the other type. Due to the periodical variation of the exchange interaction, the $Mn^{3+}-O^{2-}-Mn^{4+}$ bond lengths with the canted parallel spins are elongated, while those with the antiparallel spin ordering are shortened. Thus, the lattice relaxation in the magnetically ordered state leads[106] to dimerizaion of the $Mn^{4+}-Mn^{3+}-Mn^{3+}$ fragments and the appearance of polarization.¶

Traditional preparative methods of the solid state chemistry are used for the synthesis of the RMn_2O_5 compounds. Thus, these compounds and also $RCrMnO_5$ and $RFeMnO_5$ isostructural to them were prepared[107–109] in the polycrystalline state by the citrate synthesis, while in another study,[110] polycrystalline samples of RMn_2O_5 (R = La, Pr, Nd, Tb, Bi) were prepared using the hydrothermal treatment of R_2O_3 oxide and $KMnO_4$ mixtures in a strongly basic medium (KOH) at 240 °C during 3 days. The RMn_2O_5 single crystals are usually prepared by growth from a solution in the $PbO-PbF_2-B_2O_3$ melt[111] or by spontaneous crystallization.[112]

Lanthanide nickelates tend to exhibit charge disproportionation of Ni^{3+} to $Ni^{(3-\delta)+}$ and $Ni^{(3+\delta)+}$ and ordering of these charge states below the metal–insulator transition temperature.[113] The appearance of polarization by a mechanism similar to that considered above for RMn_2O_5 is expected[114] for the $RNiO_3$ nickelate with collinear spin ordering according to the type ↑↑↓↓.[115] However the magnetoelectric properties of $RNiO_3$ have not still been con-

¶ The ordering of the magnetic moments on the lanthanide ions is not considered in this case.

firmed. The high sensitivity of the physical properties, including the metal–insulator transition in the lanthanide nickelates to the external pressure may be crucial for the search for polarization in these compounds. The two-dimensional epitaxial compression and tensile stresses in $RNiO_3$ thin films[116] and substitution of other lanthanide ions for some R^{3+} ions with the possibility of controlled distortion of the perovskite structure open up additional ways for the strong influence on the electric properties of nickelates.[117,118] Hence, more detailed investigation of thin epitaxial films of $RNiO_3$ nickelates and $(R,R')NiO_3$ solid solutions for the appearance of polarization may be a possible way of the search for multiferroics.

Thus, one mechanism of origination of the ferroelectricity in a magnetically ordered crystals requires simultaneously:

— periodic charge variation in some chain of lattice ions $M^{n+}-O^{2-}-M^{(n+1)+}$;

— existence of a collinear system of spins with competing ferro- and antiferromagnetic exchange between ions in the same chain (giving rise to spin ordering, *e.g.*, ↑↑↓↓).

These conditions are met for $Ca_3Co_2O_6$, which is isostructural to K_4CdCl_6. The crystal structure of $Ca_3Co_2O_6$ is composed of CoO_6 trigonal prisms and CoO_6 octahedra connected along the *c* axis, these one-dimensional magnetic chains are separated by Ca^{2+} ions. As some cobalt ions in this structure are replaced by Mn^{4+} ions, the latter occupy only octahedral sites, thus forming chains of alternating Mn^{4+} and Co^{2+} ions in 1:1 ratio. The solid solution $Ca_3Co_{2-x}Mn_xO_6$ with $x = 0.96$ actually passes to the ferroelectric phase below $\sim$17 K.[119] This example confirms the possibility to predict the appearance of polarization in magnetically ordered ionic crystals when their crystal structure is known. According to a method for the preparation of single crystals of $Ca_3Co_2O_6$,[120] a 1:7 (by mass) mixture of $Ca_3Co_4O_9$ and K_2CO_3 was heated to 880 °C and kept for 48 h in air and then cooled at a rate of 100 K h^{-1}; this gave rise to needle-like crystals several millimetres long. The solid solutions $Ca_3Co_{2-x}Mn_xO_6$ were synthesized in a similar way.[119]

9. Copper-containing multiferroics

Among multiferroics, there is a series of copper-based compounds with a frustrated spin structure, which is indirectly responsible for the ferroelectric properties. One of the best studied is the lithium compound $LiCu_2O_2$ having an orthorhombic structure in which linear double $Cu^{2+}O_2$ chains separated by Li^+ and Cu^+ ions can be distinguished (see Fig. 1).[121] This compound is a typical representative of so-called quasi-one-dimensional $S = 1/2$ systems; this makes the discovery of polarization ($T_C \approx 23$ K) accompanied by magnetic ordering as a spiral spin structure in this compound even more surprising.[122] Yet another compound is $LiCuVO_4$, which crystallizes in a distorted inverted spinel structure (space group *Imma*). As in $LiCu_2O_2$, the Cu^{2+} ions form CuO_2 chains parallel to the crystallographic *c* axis having a complex magnetic structure.[123] Nevertheless, together with the antiferromagnetic structure, polarization along the *a* axis appears in $LiCuVO_4$ at much lower temperatures ($T_C < 3$ K) than in $LiCu_2O_2$.[124,125] Moreover, copper(II) oxide was also found to be a multiferroic with $T_C = 230$ K, the ferroelectricity being observed in it at temperature not lower than 215 K.[126] This is related to the destruction of the spiral spin structure and transition to the collinear antiferromagnetic phase. A distinctive feature of CuO is the Cu–O–Cu bond angle ($\varphi = 146°$), which markedly exceeds the corresponding angle in $LiCu_2O_2$ ($\varphi = 93°$) and corresponds to the value at which the ferromagnetic interaction is presumably replaced by the antiferromagnetic one.[126] This brings about the spin frustration effect and probably establishes the spiral magnetic structure, which allows polarization to arise (see Fig. 1). For $LiCu_2O_2$, the Cu–O–Cu bond angle does not provide the required frustration, which is responsible for the transition to the ferroelectric phase occurring only at very low temperature. Note that the monoclinic structure is stable for CuO, whereas other MO oxides (M = Mn, Fe, Co, Ni) crystallize in the NaCl structure. Studies of the growth of copper oxide thin films showed the possibility of epitaxial stabilization of CuO in the tetragonally distorted NaCl structure.[127] This is indicative of a small Gibbs energy (ΔG) of the polymorphic transition of CuO from the monoclinic to tetragonal phase. Note that the polymorphic transitions in the opposite direction (from the NaCl structure to the monoclinic CuO structure) for other transition metal oxides MO should also be characterized by small positive ΔG values, and these monoclinic phases can in principle be stabilized using the epitaxial growth of thin and ultrathin films of MO on appropriate substrates. In the case where the ΔG value for the transition exceeds the Gibbs energy gain caused by the epitaxy at the film/substrate interface and the unstable polymorph cannot be synthesized, then epitaxial stabilization can be successfully used to extend considerably the homogeneity region of the solid solutions based on the phase in question and doping components.[25]

Apart from copper(II) oxide, copper(II) chloride is also a multiferroic. This compound crystallizes in a CdI_2 type structure, which can be represented as planar chains composed of the $CuCl_4$ squares lying in the *bc* plane. The mechanism of appearance of the polarization and T_C of the transition to the ferroelectric phase were found to be similar to those of $LiCu_2O_2$.[128]

10. Magnetoelectric hexaferrites

Alkaline earth metal hexaferrites of Y-, M- and Z-types behave as multiferroics. In the hexaferrite $Ba_{0.5}Sr_{1.5}Zn_2Fe_{12}O_{22}$ (Y type, space group $R3m$, $Z = 3$) the single crystals of which were prepared from a $Na_2O-Fe_2O_3$ melt,[129] polarization arises in an external magnetic field ($\sim$1 T) directed along the *c* axis; any type of polarization is possible depending on the magnetic field vector.[130] The compound $Ba_2Mg_2Fe_{12}O_{22}$ (Y-type, space group $R3m$) tends to show ferrimagnetic ordering below 553 K, while below 195 K, a helical spin spiral, which forbids polarization, appears (see Fig. 1). The application of a magnetic field of only 10^{-2} T cants the conical spins structure having no inversion centre, and polarization appears.[131,132] This large difference between the magnetic field strengths that induce the transition to the ferroelectric phase in these two hexaferrites is likely to be due to the weak anisotropy of the spin structure of the latter compound ($Ba_2Mg_2Fe_{12}O_{22}$). In the structure of $Ba_{0.5}Sr_{1.5}Zn_2Fe_{12}O_{22}$, a substantial weakening of the magnetic anisotropy was also observed upon partial replacement of iron(III) by aluminium ions (up to 8 at.%).[133] The polarization was then induced in $\sim 10^{-3}$ T magnetic fields, which is an order of magnitude lower than in $Ba_2Mg_2Fe_{12}O_{22}$. Presumably, the Al^{3+} ions, which occupy octahedral sites together with the Fe^{3+} ions, decrease the deformation of the oxygen octahedra caused

by the displacement of Fe^{3+} from the centrosymmetric position and thus decrease the energy of magnetic anisotropy.[133] As a consequence, magnetic moment can be easily diverted from plane *ab* by the magnetic field applied. Meanwhile, the introduction of zinc to $Ba_2Mg_2Fe_{12}O_{22}$ to replace magnesium has destabilized the spin structure required for ferroelectricity to be manifested and, hence, has decreased the electric polarization in the crystals of $Ba_2(Mg_{1-x}Zn_x)_2Fe_{12}O_{22}$ to zero at $x = 0.4$.[134] Among Z-type hexaferrites, only $Ba_2Mg_2Fe_{12}O_{22}$ has a planar ferrimagnetic structure at room temperature.[135] When strontium is substituted for barium, the Fe–O–Fe bond angle changes, this induces magnetic frustrations and, presumably, stabilizes the spiral spin ordering.[136, 137] With the assumption of strong spin frustrations, Ishiwata *et al.*[131] studied in detail the magnetoelectric properties of $Sr_3Co_2Fe_{24}O_{41}$. It was shown that oxygen-stoichiometric specimens need to be prepared: the leakage currents in the polycrystalline specimens obtained by the solid-phase synthesis in air were three orders of magnitude higher that those synthesized in oxygen. This is due to the appearance of Fe^{2+} ions in the partially reduced hexaferrite and the subsequent appearance of the electronic conductivity along the $Fe^{2+}-O^{2-}-Fe^{3+}$ bonds. The study of $Sr_3Co_2Fe_{24}O_{41}$ showed the presence of polarization at room temperature induced by the applied magnetic field, the polarization value passing through a maximum at $B \approx 0.25$ T.[131] Further increase in the magnetic field resulted in the transition to the ferrimagnetic state with destruction of the ferroelectric ordering. This attests to a relatively low energy barrier; when it is overcome, the magnetic structure of $Sr_3Co_2Fe_{24}O_{41}$ becomes similar to the ferrimagnetic structure of $Ba_3Co_2Fe_{24}O_{41}$. Attention is attracted by the similarity of the magnetization curves and the magnetoelectric effects of $Sr_3Co_2Fe_{24}O_{41}$ and $Ba_2Mg_2Fe_{12}O_{22}$, which was attributed to the presence of identical crystal structure regions, presumably responsible for polarization, in Z- and Y-type hexaferrites.

Yet another example of material where spin frustrations are caused by chemical doping is $BaFe_{12-x}Sc_xO_{19}$ having an M-type structure. It is known[138, 139] that scandium doping of $BaFe_{12}O_{19}$ results in the transition from ferrimagnetic structure to a longitudinal conical spin structure. For investigation of the magnetoelectric behaviour of hexaferrite, $BaFe_{12-x-\delta}Sc_xMg_\delta O_{19}$ single crystals ($\delta = 0.05$), to which magnesium was added to prevent the formation of Fe^{2+} and thus to decrease the electrical conductivity, was prepared by zone melting in oxygen at 10 atm.[140] The hexaferrite $BaFe_{12-x-\delta}Sc_xMg_\delta O_{19}$ has a ferrimagnetic ordering up to temperature markedly above the room temperature; however, below some temperature, the ferrimagnetic spin structure starts to be transformed into the conical structure. The temperature of this transition depends on the degree of scandium substitution for iron to reach a maximum (370 K) at $x = 1.75$. As in the other considered hexaferrites, polarization of $BaFe_{12-x-\delta}Sc_x.Mg_\delta O_{19}$ measured at low temperature appears in an applied magnetic field as a result of transformation of the spin structure from the longitudinal conical to the inclined conical structure. Despite the actions taken to decrease the electronic conductivity, Tokunaga *et al.*[140] failed to measure directly the polarization and the magnetoelectric effect at room temperature due to high leakage currents.

11. Other spin-frustrated multiferroics

The mineral hubnerite ($MnWO_4$) has a monoclinic crystal structure (space group $P2/c$) composed of the $Mn^{2+}O_6$ and WO_6 octahedra, which share oxygen atoms and form zigzag-like chains along the crystallographic axis *c* (see Fig. 1).[141] According to neutron X-ray diffraction studies,[142] in the temperature range of 8–12.3 K, elliptical spiral spin ordering is present in $MnWO_4$, while below 8 K and in the 12.3–14 K range, collinear antiferromagnetism is found. Pyroelectric current measurements in $MnWO_4$ single crystals showed spontaneous polarization along the crystallographic axis *b* in the temperature range of 7.6–12.7 K and a zero external magnetic field, the value of this polarization being almost an order of magnitude higher than that observed for the $RMnO_3$ perovskites (R = Tb, Dy).[143] On application of the magnetic field, the polarization along the *b* axis decreased to zero and that along the *a* axis sharply increased at $B > 10$ T. Thus, $MnWO_4$ became the first multiferroic devoid of 4f elements where polarization is a consequence of the presence of a certain magnetic order.[143, 144] In the isostructural $CoWO_4$, the Co^{2+} ions have an orbital moment and a noticeable magnetic anisotropy, which is a reason for establishing of the collinear antiferromagnetic order. Conversely, in $MnWO_4$, the magnetic anisotropy energy of Mn^{2+} ions is comparable with the Dzyaloshinskii–Moriya interaction energy, which causes strong frustrations of the magnetic system and promotes the formation of a spiral spin order.[145] The partial replacement of manganese by cobalt in the $MnWO_4$ structure resulted in a considerable decrease in the polarization.[146] In iron-doped $Mn_{1-x}Fe_xWO_4$, the ferroelectric phase was already completely destroyed at $x = 0.1$.[147] The iron(II) ions stabilize the collinear antiferromagnetic ordering; however, in an applied magnetic field, the collinearity of the spin structure was destroyed, and the compound $Mn_{0.96}Fe_{0.04}WO_4$ had a high polarization, which was not inferior to the polarization of $MnWO_4$.[148] When considering the synthesis of the $MnWO_4$ phase, two most frequently used methods can be distinguished: growth of $MnWO_4$ single crystals from solution in a Na_2WO_4 melt containing $MnCO_3$ and WO_3 at 1250 °C [111, 144] and zone melting of the specimens pressed from a mixture of $MnCO_3$ and WO_3 powders annealed at 1050 °C (for 60 h under nitrogen).[144]

The orthorhombic crystal structure of the vanadates $M_3V_2O_8$ (M = Ni, Co, Mn, Zn, Cu) (space group *Cmca*) consists of layers of $M^{2+}O_6$ octahedra perpendicular to the *b* axis and separated by non-magnetic $V^{5+}O_4$ tetrahedra. In the MO_6 layers, M^{2+} ions are arranged according to the Kagome lattice pattern with the difference that the layers themselves are not planar but corrugated (Kagome staircase) (see Fig. 1). The magnetic ions in this structure can be arranged in two crystallographically non-equivalent positions, either at the common vertices that connect the triangles occurring in one plane (M1) or at the bases of the triangles that lie in different planes (M2).[149] The pronounced spin frustrations in $Ni_3V_2O_8$ give rise to high- and low-temperature incommensurate magnetic structures, which exist below 9.1 and 6.3 K, respectively; below 3.9 K, $Ni_3V_2O_8$ passes to the spin-inclined antiferromagnetic state.[150] The electric polarization was found below ~6 K and in the absence of a magnetic field, it persisted down to ~4 K. In a magnetic field ($B = 1.5–2$ T) applied along the *b* axis, the $Ni_3V_2O_8$ single crystals underwent transition from the incommensurate spin structure to the spin-inclined

state, which destroyed the ferroelectric phase; however, upon application of the field parallel to the *a* axis, polarization increased and the temperature range of its existence was extended.[151] The isovalent replacement of some Ni^{2+} ions by zinc ions (< 0.1 at.%) strongly suppressed the magnetic ordering.[152] The application of a hydrostatic pressure (~1.6 GPa) completely removed polarization in $Ni_3V_2O_8$.[153] To our knowledge, in the case of isostructural compounds $M_3V_2O_8$ (M = Mn, Ni, Co), the magnetic ordering does not disrupt the spatial inversion and, hence, cannot serve as the source of polarization. The single crystals of $Ni_3V_2O_8$ were synthesized from a solution in a $BaO-V_2O_5$ or KVO_3 melt;[154,155] for $Mn_3V_2O_8$, a $MoO_3-V_2O_5-MnO$ melt was used (1200 °C).[155] The single crystals of $Ni_3V_2O_8$, which incongruently melted at 1210 °C, were prepared[156] by growth from a solution in a V_2O_5 and $SrCO_3$ mixture melt (molar ratio 2 : 3) combined with zone melting.

Delafossites are compounds with the general formula $A^+B^{3+}O_2$ (A = Ag, Cu, Pd, Pt; B = Al, Cr, Fe, Co, Ni, Ga, Rh, In) crystallizing in the rhombohedral (*R*3*m*) or hexagonal (*P*6/*mmc*) polytypes, which differ by the sequence of layers: AaBbCcAa... and AaBbAa... (A, B, C are the layers of cations A; a, b, c are layers of distorted BO_6 octahedra) (see Fig. 1).[157,158] The two-dimensional lattice with a triangular arrangement of B^{3+} magnetic ions in the *ab* plane is a source of strong spin frustrations; in this respect, delafossites are similar to hexagonal lanthanide manganites. In the parent delafossite, $CuFeO_2$ (space group *R*3*m*), a collinear spin ordering according to the ↑↑↓↓ pattern along the [110] direction is established below ~11 K and is transformed to a spiral spin structure in a 7–13 T magnetic field applied along the *c* axis. This brings about the polarization $P_s \sim 200-400$ μC m^{-2} the vector of which lies in the *ab* plane.[159]

Minor doping with aluminium (about 2 at.% Al in the Fe sublattice) changes appreciably the magnetic structure of $CuFeO_2$: the spin spiral and electric polarization appear even in the absence of a magnetic field.[160,161] Doping of $CuFeO_2$ with gallium (3.7 at.%) produced a similar result: polarization (~250 μC cm^{-2}) was observed below 7.5 K.[162] In the series of $CuFe_{1-x}Rh_xO_2$ solid solutions ($0.02 < x < 0.15$), the ferroelectric phase was stable at $T < 8$ K for $x = 0.08$.[163] A study of the magnetoelectric properties of the delafossites $ACrO_2$ (A = Cu, Ag) showed that the electric polarization appears in these compounds below ~25 K together with establishing of the spiral spin ordering, which implies a strong relationship between the electric and magnetic subsystems.[164] Conversely, transition of $LiCrO_2$ and $NaCrO_2$ (distorted NaCl structure) to the spin-spiral state is not accompanied by the appearance of polarization; however, as the Néel temperature has been passed, the dielectric constant changes jumpwise, which may be related to transition to the antiferroelectric phase.[165] It is of interest that ferroelectric ordering occurs also for the layered chalcogenide $AgCrS_2$ (space group *R*3*m*) below ~43 K. Note that despite the similar layered crystal structures of $AgCrS_2$ and delafossite $AgCrO_2$, the coordination environments of the silver atoms in these compounds are different, so are the types of chromium polyhedra: CrS_6 is an asymmetric trigonal prism and CrO_6 is an octahedron.[166] The $CuCrO_2$ single crystals are grown from a solution in a Bi_2O_3 melt.[164] The single crystals of $CuFeO_2$ and the solid solutions based thereon are usually obtained by zone melting from $Cu_2O + Fe_2O_3$ or $2\,CuO + Fe_2O_3$ mixtures.[167] The polycrystalline specimens of some Ag- and Cu-containing delafossites that are unstable at high temperature can be prepared from more stable Na- and K-containing compounds $A^+B^{3+}O_2$ by ion exchange with silver and copper salt melts.[168–170] A technological challenge is the preparation of delafossites as epitaxial thin films.[158] The epitaxial growth of delafossites is usually performed with single crystalline substrates such as sapphire (c- and R-cuts), cubic (111)$ZrO_2(Y_2O_3)$, and (111)$MgAl_2O_4$.[158,171,172] Additional preparative possibility of potential increase in the number of the synthesized delafossites is opened by the epitaxial stabilization, an example being provided by thin films of the $CuInO_2$ phase, which is metastable in the bulk state.[173] The biaxially strained thin films of multiferroic delafossites can differ from the single crystals by physical properties. Detailed investigation of the magnetoelectric interactions in them could clarify the origin of magnetically induced polarization in delafossites.

Some compounds with the spinel structure also proved to be multiferroic. For example, the transition of $CoCr_2O_4$ from the ferrimagnetic to conical spin structure at ~25 K is accompanied by the appearance of spontaneous polarization.[174] The low polarization values (~2 μC m^{-2}) are attributable to the weak spin–orbit coupling typical of Cr^{3+} unlike Mn^{3+} ions, which undergo strong spin–orbit coupling in the perovskites $RMnO_3$. Direct relationship between the polarization and the magnetic subsystem in $CoCr_2O_4$ was confirmed by measuring the hysteresis $P(H)$ (H is the magnetic field strength) and time-synchronized reversal of polarization in phase opposition with the varying magnetic field.[175] Rather recently, a new multiferroic with the spinel structure, CdV_2O_4, was reported.[176] The key distinction of CdV_2O_4 from $CoCr_2O_4$ is the magnetic structure with spin ordering according to the ↑↑↓↓ pattern along the [101] and [011] directions similar to the ordering in the perovskite lanthanide nickelates. In CdV_2O_4 specimens obtained by solid-state synthesis, the expected transition from the cubic to tetragonal phase occurs at 95 K and transition to the magnetically ordered state occurs at 33 K. The formation of the collinear antiferromagnetic order was accompanied by the simultaneous transition to the ferroelectric phase the polarization of which reached 5 μC m^{-2}, which is higher than the spontaneous polarization observed in $CoCr_2O_4$. Note that for the isostructural compounds MV_2O_4 (M = Zn, Mg), no ferroelectric ordering was detected.[176] In terms of the nature of the arising ferroelectricity, CdV_2O_4 is identical to the above-considered $Ca_3Co_{2-x}Mn_xO_6$ and $LnMn_2O_5$ (Ln = Dy, Tb): an electronic instability connected directly to the ↑↑↓↓ type spin ordering appears in the structure, resulting in V–V bond dimerization with simultaneous elongation and shortening of the V–O bonds, which in turn brings about the electronic polarization.[176]

The structural abundance of the existing multiferroics is supplemented by silicate-based pyroxenes, which are minerals described as $AMSi_2O_6$, where A is a mono- or divalent metal and M is a di- or trivalent metal. Pyroxenes crystallize in orthorhombic or monoclinic system and are composed of layers of SiO_4 tetrahedra and MO_6 octahedra, which alternate in such a way that the zigzag-like chains of MO_6 octahedra run along the *c* axis and are connected in the (110) and ($\bar{1}$10) planes by chains of the SiO_4 tetrahedra (see Fig. 1).[177] If the cations M have unpaired spins, then a magnetic structure with a triangular arrangement of the

magnetic moments in the (110) planes arises in the quasi-one-dimensional chains of MO_6 octahedra; this serves as the source of geometric spin frustrations in pyroxenes.[178] The ferroelectric ordering was found in $LiFeSi_2O_6$, $LiCrSi_2O_6$ and $NaFeSi_2O_6$ below 18, 11 and 6 K, respectively; it was shown that polarization depends strongly on the magnitude and direction of the applied magnetic field.[178] These results were confirmed subsequently by other researchers.[179] There is still no unambiguous answer to the question of how polarization arises in the magnetically ordered pyroxene phase.

Apart from the above-described multiferroics found among complex oxides, other, less popular single-phase compounds with potential magnetoelectric behaviour also exist. For example, multiferroic properties were detected in $Ba_2LnFeNb_4O_{15}$ (Ln = Nd, Sm, Eu) with the tetragonal tungsten bronze structure [180] and in $RbFe(MoO_4)_2$,[181] $FeTe_2O_5Br$,[182] Fe_2OBO_3,[183] $Ba_2CoGe_2O_7$,[184] $Ga_{2-x}Fe_xO_3$,[185] $FeVO_4$,[186] Cr_2BeO_4,[187] $RCrO_3$ (R = Lu, Yb, Er, Ho, Y)[188] and in the lanthanide ferroborates $RFe_3(BO_3)_4$.[189] Due to the limited space, we do not consider the characteristic features of these compounds but would like to emphasize that for most of them the presence of magnetoelectric properties has to be confirmed.

12. Multiferroics based on fluorides

The magnetic ferroelectrics based on fluorides have been considered in detail in a review [190] devoted to various non-oxide multiferroics. We shall restrict our consideration to brief information on the existing fluorine-containing magnetoelectrics. The first group includes compounds with the general formula $BaMF_4$ (M = Mn, Ni, Fe, Co), which crystallize in the orthorhombic system with space group $A2_1am$.[191] The two-dimensional ferroelectric ordering was identified [192] in $BaNiF_4$ and $BaCoF_4$ with Curie temperatures above the melting points of the compounds (about 1100–1300 K), whereas the other compounds, $BaFeF_4$ and $BaMnF_4$, are pyroelectrics. The crystal structure of the $BaMF_4$ family contains layers of edge-sharing MF_6 octahedra separated by layers of Ba^{2+} cations. Polarization is established along the *a* axis being a consequence of displacement of the Ba^{2+} cations along the *c* axis with simultaneous rotation of the MF_6 octahedra in the *ab* plane.[193] The antiferromagnetism in $BaMF_4$ is established at the Néel temperature ranging from ~30 to 80 K in the series M = Mn, Fe, Co, Ni.[194, 195]

A number of publications are devoted to the study of $K_3Fe_5F_{15}$ (space group *Pba*2) in which the iron ions in different oxidation states are present (+2 and +3). This compound is magnetoelectric with ferroelectric and magnetic transition temperatures of 490 and 125 K, respectively.[196, 197] Presumably, the polarization in $K_3Fe_5F_{15}$ is related to the displacement of Fe^{2+} and Fe^{3+} cations arranged in an ordered fashion in octahedral positions, whereas above the Curie temperature, the different-valence iron ions are disordered in the crystal structure and are located at the centres of the octahedra.[198] The polycrystalline fluorides are synthesized from a stoichiometric mixture of KF, FeF_2 and FeF_3 in sealed golden tubes at ~750 °C for 15 h. The small single crystals of $K_3Fe_5F_{15}$ are formed upon long-term (about 15 days) recrystallization of polycrystalline specimens in the same tube at ~750 °C. The single crystals of the $BaMF_4$ phase are obtained from a BaF_2 and MF_2 melt in an HF atmosphere at ~800 °C.[195] A low-temperature hydrothermal synthesis of special-purity polycrystalline $BaMF_4$ (M = Mg, Mn, Co, Ni, Zn) from BaF_2, MF_2, CF_3CO_2H and H_2O was also proposed; the synthesis is carried out at 230 °C for 24 h.[199]

13. Multiferroics based on organic compounds

In recent years, new multiferroics have been discovered among the transition metal complexes with organic ligands and other compounds containing organic moieties where polarization is induced by proton transfer. Thus in the perovskite-like structure of the formate complexes $(Me_2NH_2)M(HCO_2)_3$ (M = Mn, Co, Ni), the MO_6 blocks appear in the perovskite B-sites and the dimethylammonium cations occupy the A-sites (Fig. 3 *a*). At temperatures below 160–180 K, the proton transfer between the $HCOO^-$ and $^+NH_2$ groups gives rise to antiferroelectricity, while below ~35 K (for M = Ni), the non-centrosymmetric bridging

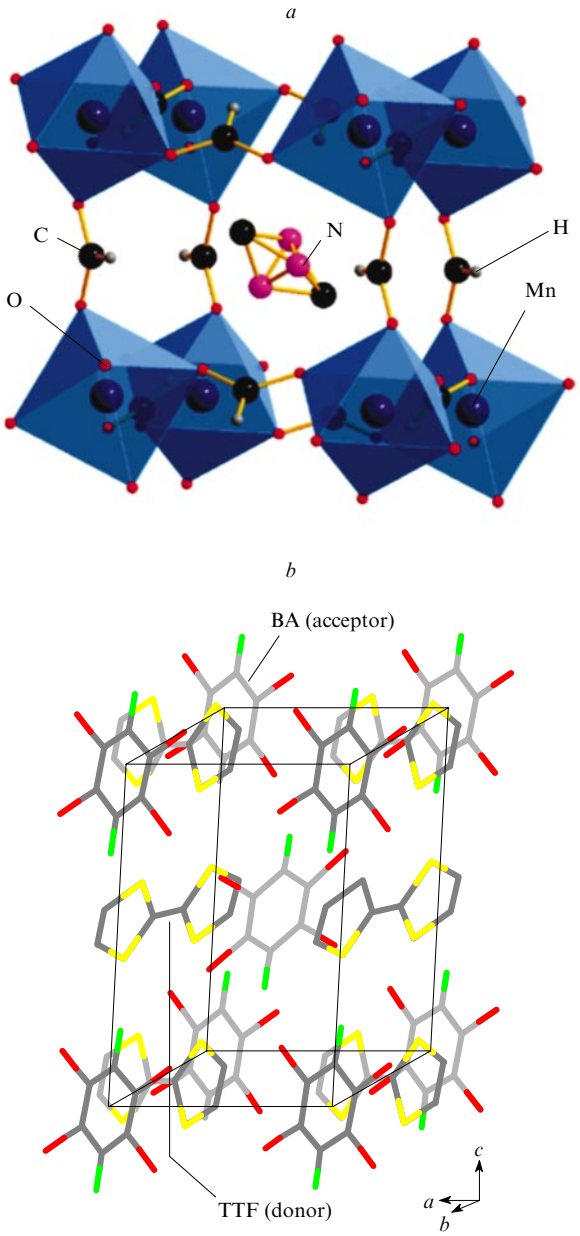


Figure 3. Multiferroic $(Me_2NH_2)Mn(HCO_2)_3$ with the perovskite topology (*a*) and crystal structure of tetrathiafulvalene–*p*-bromanil (*b*).[4]

μ-HCO_2^- groups that link the metal ions skew the Ni spins, and the compound acquires weak ferromagnetism.[5] In another compound with the perovskite topology, $(EtNH_3)_2CuCl_4$, polarization was found below $\sim$270 K ($P_s \approx 18$ μC cm^{-2}), which arises due to weak hydrogen bonding between the $EtNH_3^+$ cations and chloride anions and the presumed reorientation of the ethylammonium groups on cooling.[200] The spins in the $CuCl_4$ planes have a ferromagnetic order below 10 K. It is noteworthy that the magnetically induced polarization was also detected in metal compounds with organic ligands, for example, in $CuCl_2 \cdot 2\,Me_2SO$ (below 1 K in 0.3–3.8 T fields).[6]

Among organic compounds, the tetrathiafulvalene–*p*-bromanil (TTF–BA, Fig. 3*b*) donor – acceptor complex is distinguished by the Peierls lattice instability along the highly ionized one-dimensional $TTF^+ - BA^- - TTF^+ - BA^- - \ldots$ chain with the spin $s = 1/2$. Dimerization of the donors and acceptors results in the formation of a spin-singlet state of the $TTF^+ - BA^-$ pairs with a weak antiferromagnetic interaction between these pairs below $\sim$50 K. The pattern of appearance of the polarization upon this spin-Peierls transition was described in a review[201] dealing with organic ferroelectrics. Indeed, it was shown experimentally that apart from dimerization, polarization (up to 0.15 μC cm^{-2}) appears in TTF–BA;[4] this value is two orders of magnitude higher than polarization in the magnetically induced multiferroics such as $TbMnO_3$.

IV. Composite multiferroics

Apart from the homogeneous multiferroics, considerable attention is also devoted to artificial (composite) multiferroics composed, most often, of two separate phases, ferromagnetic and ferroelectric ones. In this approach, the magnetic and ferroelectric ordering temperatures and other magnetic and ferroelectric characteristics are determined by the choice of the phases that form the composite. The magnetoelectric composites were considered in detail in recent reviews;[202–205] therefore, we shall restrict ourselves only to the description of existing material science approaches to the design of these materials and shall also touch upon some related problems. Composite multiferroics are usually classified into bulk and thin-film ones and in terms of the type of internal geometry of component arrangement: alternating layers of the components (type 1), columnar structures in a matrix (type 2) and granular inclusions of one component in the matrix of the other component (type 3).[203]

1. Bulk magnetoelectric composites

Bulk composites usually include ceramic-, alloy- and/or polymer-based components. For materials containing ceramic components [*e.g.*, piezoelectric $Pb(Zr,Ti)O_3$ (PZT) and ferrimagnetic $NiFe_2O_4$] in a mixed form (type 3), the key unsolved problem is minimization of the chemical interaction and uncontrolled mutual doping of the phases that form the composite during its high-temperature sintering. High leakage currents caused by the electrical conductivity at grain boundaries and often the metallic properties of the magnetic phase together with the insufficient quality of the mixed powders result in the measurable magnetoelectric effect values being lowered by a factor of tens as compared with the theoretically predicted value. Note also that for high magnetoelectric effect to be achieved, a composite with clear-cut interfaces and the maximum contact surface area of the two phases needs to be obtained. Furthermore, there is the problem of disorientation of the crystallites of the magnetic phase in the ferroelectric matrix, which often reduces the magnetoelectric effect. An interesting way of increasing the surface area between the phases is the preparation of core–shell particles[202,206] with subsequent sintering of the particles (only shells rather than cores are sintered together). When producing layered composites (type 3), magnetic ceramic phases are often replaced by magnetic alloys such as $Tb_{1-x}Dy_xFe_2$ (Terfenol-D); polymers are used, most often, as binders.[202–204]

2. Thin-film composites

Composites with a particular orientation of the crystallites in the ferroelectric matrix can be easily manufactured by the epitaxial on-substrate growth of the matrix. In thin films, the composite multiferroics can have any of the three key types of internal geometry. The first type, *i.e.*, the laminate structure, is created by successive growth of the ferroelectric and/or magnetic phase from either gas phase or solution[207] on single-crystalline substrates, which can also act as one of the composite components. Note, however, that the magnetoelectric interface bonding decreased in this case due to the too strong epitaxial intergrowth of the ferroelectric phase with the substrate.[208]

Rather recently, the possibility of creating thin-film magnetoelectric materials based on nanopillars was demonstrated.[209] By choosing the components that spontaneously crystallized in two separate immiscible phases (*e.g.*, perovskite and spinel phases[210]), it is possible to obtain nanopillars of one phase embedded in the matrix of the other phase. This geometry and the typical pillar diameter (tens of nanometres) ensure the high interfacial area-to-phase volume ratio, which is an important parameter needed to be taken into account for coupling of two materials *via* mechanical stress. Moreover, in this type of nanocomposites, the operating magnetoelectric interface is perpendicular to the substrate, which considerably reduces clamping of the ferroelectric layer by the substrate and thus increases the efficiency of mechanical coupling of the magnetic and ferroelectric phases.

The third type of internal geometry of the thin film composites can be implemented in the case where the unit cell parameters in the section plane of the single crystalline substrate would be perfectly suitable for the coherent growth of only one phase and have a strong parameter mismatch with the other phase. The thin-film nanocomposites of this type were first obtained in our study.[211] The composite components were ferromagnetic perovskite $Pr_{0.7}Sr_{0.3}MnO_3$ and ferroelectric $LuMnO_3$ with hexagonal structure. In the $Pr_{0.7}Sr_{0.3}MnO_3 - LuMnO_3$ films grown on the $(111)ZrO_2(Y_2O_3)$ and (111)MgO substrates, phase separation occurred: the expected epitaxial growth of the hexagonal $LuMnO_3$ matrix took place, while the perovskite $Pr_{0.7}Sr_{0.3}MnO_3$ phase was present in the composite as $\sim$20 nm granular inclusions (Fig. 4).[211] Note also the strong coupling of the ferromagnetic and ferroelectric components through the mechanical subsystem that we found in this composite. Note that the magnetoelectric effect in these composites should be maximum when the percolation threshold of the nanoinclusions in the epitaxial matrix has been reached (Fig. 5). However, the successful development of this type of composite multiferroics is still held up by the mutual doping of the matrix and the

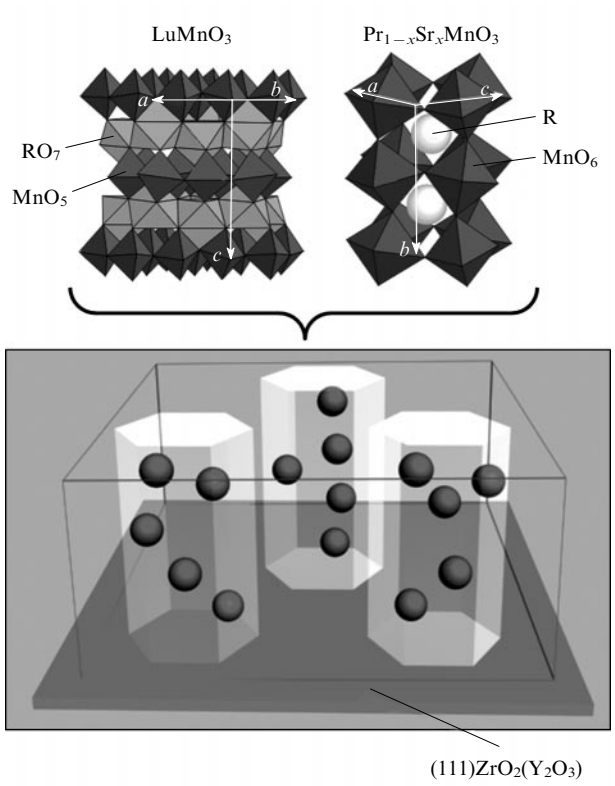


Figure 4. Scheme of formation of the magnetoelectric nanocomposite $Pr_{0.7}Sr_{0.3}MnO_3-LuMnO_3$.[211]

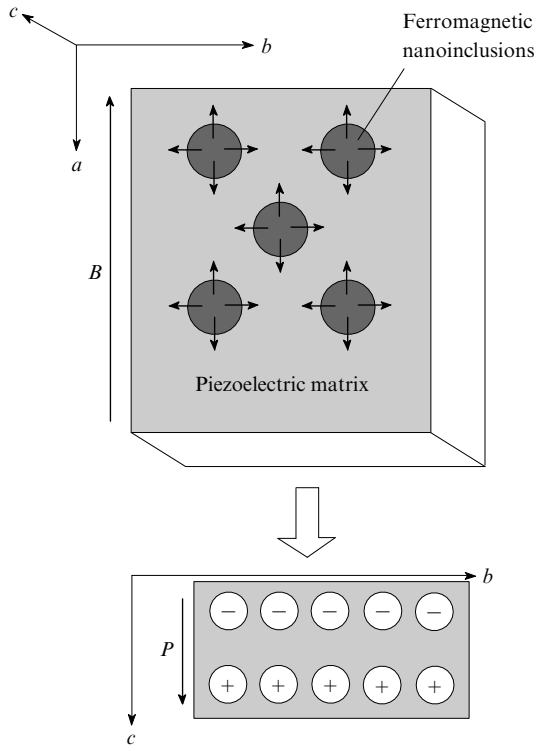


Figure 5. Scheme of operation of the magnetoelectric composite material.

inclusions, and only rarely, their interaction is low enough to have no pronounced effect on the properties of both phases.

V. Conclusion

This review is an attempt to cover as fully as possible the existing variety of multiferroics and briefly describe those that are of most interest as regards the mechanism of origination of the coupling between the electric and magnetic types of ordering. The crystal chemical features of these materials and the methods for their synthesis are considered. The multiferroic subject is tightly connected with complex, often poorly studied, physical processes in crystals; therefore, it was necessary to consider the characteristic physical properties of these compounds.

In the case of single-phase multiferroics with separately existing magnetic and ferroelectric ordering, the magnetoelectric effect is most often much inferior to this effect in magnetically induced ferroelectrics and composite magnetoelectrics. For multiferroics where polarization is expected as a consequence of the magnetic order, the crystal structure should ensure either strong spin frustrations for establishing of a certain spin order disrupting the spatial inversion of the crystal or charge ordering with simultaneous definite antiferromagnetic order, which is often achieved by chemical doping (for example, $Ca_3Co_{2-x}Mn_xO_6$).

A promising way of the synthesis of new multiferroics is epitaxial stabilization of phases not existing in the bulk, for example, hexagonal $DyMnO_3$, hexagonal lanthanide ferrites and so on. The review demonstrates also another approach: development of mechanical stresses in the quantum paraelectric crystals. Every now and then publications appear that are devoted to the prediction of polarization along with the existing magnetic order in these crystals (*e.g.*, EuO, $SrMnO_3$). We would like to draw attention of experimentalists to this approach as one of the most promising one for the development of new multiferroics.

It is reasonable to expect that new multiferroics and new physical mechanisms of interaction of magnetic and ferroelectric orderings will be discovered in the future. Due to the lack of publications, we did not touch upon the hypothetical approaches to the design of magnetoelectrics such as molecular beam epitaxial deposition of magnetoelectric interfaces and magnetoelectric superstructures. However, it is obvious that these approaches could considerably extend the list of known multiferroics and open up new mechanisms of coupling of ferro-orderings that have not yet been experimentally discovered.

Despite lots of new ideas and achievements that appeared in recent years in the field of design of composite multiferroics, many challenges are still waiting to be solved, in particular some fundamental problems. The charge and spin effects at the interfaces between components, which substantially affect the magnetoelectric properties, have not been adequately studied as yet. The development of new high-tech solutions in such fields as nanoelectronics requires the design of nanocomposites with the sizes of crystallites of different phases are about 10 nm. Thus, there is high demand of new approaches to the controlled synthesis of bulk magnetoelectrics with high crystal quality of the neighbouring phases and interfaces and to the development of new and optimization of existing methods for the preparation of thin-film composites as most demanded in the modern electronics and spintronics.

This review was prepared with the financial support from the Russian Foundation for Basic Research (Project No. 10-03-00964).

VI. Appendix

Table. Structural features and properties of some multiferroics.

Compound	Structure	Magnetic ordering	Ferroelectric ordering	Comments	Ref.
$BiFeO_3$	perovskite	cycloidal AFM with $\lambda = 62$ nm (locally G-type), $T_N = 643$ K	FE, $T_C = 1103$ K	polarization appears due to ordering of the $6s^2$ electron pairs on Bi^{3+} ions	212, 213
$Ni_3B_7O_{13}I$	boracite	120 – 64 K: AFM, below 64 K; weak FM	120 – 64 K: piezoelectric, below 64 K: FE	–	43
$LiNiPO_4$	olivine	AFM, $T_N \approx 20$ K	FE, $T_C \approx 20$ K	the FE phase appears in $B < 12$ T fields in the presence of the commensurate AFM structure	51
$EuTiO_3$	perovskite	FM, $T_C = 4.2$ K	FE, $T_C = 250$ K	biaxial strains in the epitaxial films caused the AFM/PE to FE/FM phase transition	54
$TbMnO_3$	"	41 – 28 K: sinusoidal AFM, below 28 K: cycloidal AFM	FE, $T_C = 28$ K	polarization appears simultaneously with the spin structure rearrangement from sinusoidal to cycloidal	11
$HoMnO_3$	hexagonal	triangular planar AFM, $T_N \approx 70$ K	FE, $T_C \approx 900$ K	improper FE ordering not related to the magnetic order	214
$LuFe_2O_4$	rhombohedral, specific case of $(RMO_3)_n(MO)_m$	presumably FM, $T_C = 240$ K	FE, $T_C = 330$ K	FE is due to the charge frustrations on a triangular lattice	14, 90
Fe_3O_4	inverted spinel	FM, $T_C \approx 860$ K	FE, $T_C = 120$ K	FE appears below the Verwey point	99
YMn_2O_5	orthorhombic	45 – 40 K: incommensurate AFM, 39 – 19 K: commensurate AFM, below 19 K: incommensurate AFM	FE at 19 – 39 K	commensurate collinear AFM ordering is responsible for the appearance of polarization	215, 216
$Ca_3Co_{2-x}Mn_xO_6$ ($x = 0.96$)	K_4CdCl_6 type	AFM, $T_N \approx 15$ K	FE below ~ 15 K	FE is caused by collinear AFM order	119, 217
$LiCu_2O_2$	orthorhombic	spiral AFM, $T_N = 23$ K	FE, $T_C = 23$ K	polarization is caused by the spiral spin structure	122, 218
$LiCuVO_4$	inverted spinel	spiral AFM, $T_N = 2.5$ K	FE below ~ 2.5 K	the same	124
CuO	monoclinic	213 – 250 K: spiral AFM below 213 K: collinear AFM	213 – 250 K: FE	"	126
$CuCl_2$	monoclinic (CdI_2 type)	cycloidal AFM, $T_N = 24$ K	FE, $T_C = 24$ K	"	128
$Ba_2Mg_2Fe_{12}O_{22}$	Y-type hexaferrite	553 – 195 K: FM, 195 – 50 K: helical spin spiral, below 50 K: longitudinal conical	FE in an external magnetic field $> \sim 1$ mT, $T_C = 195$ K	polarization is caused by the presence of canted conical spin structure that appeared due to magnetic field-induced transformation of the initially helical spiral	131

Table (continued).

Compound	Structure	Magnetic ordering	Ferroelectric ordering	Comments	Ref.
$MnWO_4$	monoclinic	12 – 8 K: elliptical AFM, 14 – 12 K and below 8 K: collinear AFM	12 – 8 K: FE	polarization is caused by the elliptical spin structure	143
$Ni_3V_2O_8$	orthorhombic	9 – 4 K: incommensurate AFM, below 4 K: spin-inclined AFM	6 – 4 K: FE below 4 4: FE in an applied magnetic field along *a* axis ($B > 3$ T)	polarization is a consequence of the presence of low-temperature incommensurate spin structure below 6 K	151
$CuFeO_2$	delafossite	collinear AFM, $T_N = 11$ K	FE, $T_C = 11$ K in a 7 – 12 T magnetic field	polarization is induced by transformation of the collinear AFM ordering to spiral ordering in $B > 7$ T fields	159
$CoCr_2O_4$	spinel	93 – 25 K: FM, beliw 25 K: conical AFM	FE, $T_C = 25$ K	polarization is caused by the presence of lateral conical spin structure	175
CdV_2O_4	"	conical AFM, $T_N = 33$ K	FE, $T_C = 25$ K	collinear AFM ordering induces polarization	176
$NaFeSi_2O_6$	pyroxene	AFM, $T_N = 8$ K	FE, $T_C = 6$ K		178
$K_3Fe_5F_{15}$	monoclinic	weak FM, $T_C = 122$ K	FE, $T_C = 490$ K		196, 197
(Me_2NH_2). .$Ni(HCO_2)_3$	perovskite-like	FM, $T_C = 35$ K	AFE below ~ 160 K	FE behaviour is due to proton transfer	5
TTF – BA	triclinic	weak FM below 53 K	FE below 53 K	polarization appears due to the spin-Peierls instability	4

Notes. AFM is antiferromagnetic, FE is ferroelectric, AFE is antiferroelectric, FM is ferromagnetic, PE is paraelectric.

References

1. H Schmid *Ferroelectrics* **162** xix (1994)
2. W Eerenstein, N D Mathur, J F Scott *Nature* **442** 759 (2006)
3. D N Astrov *Zh. Eksp. Teor. Fiz.* **40** 1035 (1961) [a]
4. F Kagawa, S Horiuchi, M Tokunaga, J Fujioka, Y Tokura *Nat. Phys.* **6** 169 (2010)
5. P Jain, V Ramachandran, R J Clark, H D Zhou, B H Toby, N S Dalal, H W Kroto, A K Cheetham *J. Am. Chem. Soc.* **131** 13625 (2009)
6. V S Zapf, M Kenzelmann, F Wolff-Fabris, F Balakirev, Y Chen *Phys. Rev. B* **82** 060402(R) (2010)
7. I S Zheludev *Pramana* **9** 385 (1977)
8. R E Cohen *Nature (London)* **358** 136 (1992)
9. C Blaauw, F van der Woude *J. Phys. C: Solid State Phys.* **6** 1422 (1973)
10. N Aliouane, O Prokhnenko, R Feyerherm, M Mostovoy, J Strempfer, K Habicht, K C Rule, E Dudzik, A U B Wolter, A Maljuk, D N Argyriou *J. Phys.: Condens. Matter* **20** 434215 (2008)
11. T Kimura, G Lawes, T Goto, Y Tokura, A P Ramirez *Phys. Rev. B* **71** 224425 (2005)
12. S Picozzi, K Yamauchi, B Sanyal, I A Sergienko, E Dagotto *Phys. Rev. Lett.* **99** 227201 (2007)
13. M Alexe, M Ziese, D Hesse, P Esquinazi, K Yamauchi, T Fukushima, S Picozzi, U Glsele *Adv. Mater.* **21** 4452 (2009)
14. N Ikeda, H Ohsumi, K Ohwada, K Ishii, T Inami, K Kakurai, Y Murakami, K Yoshii, S Mori, Y Horibe, H Kitô *Nature (London)* **436** 1136 (2005)
15. J R Teague, R Gerson, W J James *Solid State Commun.* **8** 1073 (1970)
16. S-C Yang, C-S Park, K-H Cho, S Priya *J. Appl. Phys.* **108** 093706 (2010)
17. F Chen, Q F Zhang, J H Li, Y J Qi, C J Lu, X B Chen, X M Ren, Y Zhao *Appl. Phys. Lett.* **89** 092910 (2006)
18. D Lebeugle, D Colson, A Forget, M Viret, P Bonville, J F Marucco, S Fusil *Phys. Rev. B* **76** 024116 (2007)
19. S T Zhang, M H Lu, D Wu, Y F Chen, N B Ming *Appl. Phys. Lett.* **87** 262907 (2005)
20. J Li, J Wang, M Wuttig, R Ramesh, N Wang, B Ruette, A P Pyatakov, A K Zvezdin, D Viehland *Appl. Phys. Lett.* **84** 5261 (2004)
21. M S Kartavtseva, O Yu Gorbenko, A R Kaul, T V Murzina, S A Savinov, O A Aktsipetrov *J. Mater. Res.* **22** 2063 (2007)
22. F Bai, J Wang, M Wuttig, J Li, N Wang, A P Pyatakov, A K Zvezdin, L E Cross, D Viehland *Appl. Phys. Lett.* **86** 032511 (2005)
23. M S Kartavtseva, O Yu Gorbenko, A R Kaul, T V Murzina, S A Savinov, A Barthélémy *Thin Solid Films* **515** 6416 (2007)
24. M S Kartavtseva, O Yu Gorbenko, A R Kaul', S A Savinov *Poverkhnost'* **2** 1 (2008)
25. A R Kaul', O Yu Gorbenko, A A Kamenev *Russ. Chem. Rev.* **73** 861 (2004)
26. M S Kartavtseva, O Yu Gorbenko, A R Kaul, A R Akbashev, T V Murzina, S Fusil, A Barthélémy, F Pailloux *Surf. Coat. Technol.* **201** 9149 (2007)
27. V R Palkar, K Prashanthi, S P Dattagupta *J. Phys. D: Appl. Phys.* **41** 045003 (2008)
28. X Chen, G Hu, W Wu, C Yang, X Wang, S Fan *J. Am. Ceram. Soc.* **93** 948 (2010)
29. D Kothari, V R Reddy, A Gupta, C Meneghini, G Aquilanti *J. Phys.: Condens. Matter* **22** 356001 (2010)
30. V A Khomchenko, V V Shvartsman, P Borisov, W Kleemann, D A Kiselev, I K Bdikin, J M Vieira, A L Kholkin *Acta Mater.* **57** 5137 (2009)
31. M Valant, A K Axelsson, N Alford *Chem. Mater.* **19** 5431 (2007)
32. Yu F Kargin, V I Burkov, A A Mar'in, A V Egorysheva *Kristally* $Bi_{12}M_xO_{20\pm\delta}$ *so Strukturoi Sillenita. Sintez, Stroenie, Svoistva* (Crystals $Bi_{12}M_xO_{20\pm\delta}$ with Sillenite Structure. Synthesis, Structure and Properties) (Moscow: Institute of Organic Inorganic Chemistry, Russian Academy of Sciences, 2004)
33. G A Smolenskii, V A Isupov, A I Agranovskaya, N N Krainik *Fiz. Tv. Tela* **2** 2982 (1960) [b]
34. V A Bokov, I E Myl'nikova, G A Smolenskii *Zh. Eksp. Teor. Fiz.* **42** 643 (1962) [a]
35. G A Smolenskii, I E Chupis *Usp. Fiz. Nauk* **137** 415 (1982) [c]
36. A Kumar, G L Sharma, R S Katiyar, R Pirc, R Blinc, J F Scott *J. Phys.: Condens. Matter* **21** 382204 (2009)
37. A Levstik, V Bobnar, C Filipič, J Holc, M Kosec, R Blinc, Z Trontelj, Z Jagličič *Appl. Phys. Lett.* **91** 012905 (2007)
38. W Kleemann, V V Shvartsman, P Borisov, A Kania *Phys. Rev. Lett.* **105** 257202 (2010)
39. D A Sanchez, A Kumar, N Ortega, R S Katiyar, J F Scott *Appl. Phys. Lett.* **97** 202910 (2010)
40. W Peng, N Lemee, J-L Dellis, V V Shvartsman, P Borisov, W Kleemann, Z Trontelj, J Holc, M Kosec, R Blinc, M G Karkut *Appl. Phys. Lett.* **95** 132507 (2009)
41. R Pirc, R Blinc, J F Scott *Phys. Rev. B* **79** 214114 (2009)
42. V A Shuvaeva, K A Lysenko, M Yu Antipin *Phys. Solid State* **53** 730 (2011)
43. E Ascher, H Rieder, H Schmid, H Stössel *J. Appl. Phys.* **37** 1404 (1966)
44. H Schmid *J. Phys. Chem. Solids* **26** 973 (1965)
45. J Ju, H Li, Y Wang, J Lin, C Dong *J. Mater. Chem.* **12** 1771 (2002)
46. S-Y Chung, J T Bloking, Y-M Chiang *Nat. Mater.* **1** 123 (2002)
47. P S Herle, B Ellis, N Coombs, L F Nazar *Nat. Mater.* **3** 147 (2004)
48. A Yamada, S C Chung, K Hinokuma *J. Electrochem. Soc.* **148** A224 (2001)
49. J M Mays *Phys. Rev.* **131** 38 (1963)
50. J Li, W Tian, Y Chen, J L Zarestky, J W Lynn, D Vaknin *Phys. Rev. B* **79** 144410 (2009)
51. T B S Jensen, N B Christensen, M Kenzelmann, H M Rønnow, C Niedermayer, N H Andersen, K Lefmann, J Schefer, M von Zimmermann, J Li, J L Zarestky, D Vaknin *Phys. Rev. B* **79** 092412 (2009)
52. J H Haeni, P Irvin, W Chang, R Uecker, P Reiche, Y L Li, S Choudhury, W Tian, M E Hawley, B Craigo, A K Tagantsev, X Q Pan, S K Streiffer, L Q Chen, S W Kirchoefer, J Levy, D G Schlom *Nature (London)* **430** 758 (2004)
53. M Tyunina, J Narkilahti, M Plekh, R Oja, R M Nieminen, A Dejneka, V Trepakov *Phys. Rev. Lett.* **104** 227601 (2010)
54. J H Lee, L Fang, E Vlahos, X Ke, Y W Jung, L F Kourkoutis, J-W Kim, P J Ryan, T Heeg, M Roeckerath, V Goian, M Bernhagen, R Uecker, P C Hammel, K M Rabe, S Kamba, J Schubert, J W Freeland, D A Muller, C J Fennie, P Schiffer, V Gopalan, E Johnston-Halperin, D G Schlom *Nature (London)* **466** 954 (2010)
55. C J Fennie, K M Rabe *Phys. Rev. Lett.* **97** 267602 (2006)
56. J H Lee, K M Rabe *Phys. Rev. Lett.* **104** 207204 (2010)
57. E Bousquet, N A Spaldin, P Ghosez *Phys. Rev. Lett.* **104** 037601 (2010)
58. M Posternak, A Baldereschi, H Krakauer, R Resta *Phys. Rev. B* **55** 15983 (1997)
59. J Junquera, P Ghosez *J. Comput. Theor. Nanosci.* **5** 2071 (2008)
60. N Iwata, G Pindoria, T Morishita, K Kohn *J. Phys. Soc. Jpn.* **69** 230 (2000)
61. H L Yakel Jr, W C Koehler, E F Bertaut, E F Forrat *Acta Crystallogr.* **16** 957 (1963)

62. B B Van Aken, A Meetsma, T T M Palstra *Acta Crystallogr., Sect. E: Struct. Rep. Online* **57** i101 (2001)
63. B B Van Aken, T T M Palstra, A Filippetti, N A Spaldin *Nat. Mater.* **3** 164 (2004)
64. T Katsufuji, M Masaki, A Machida, M Moritomo, K Kato, E Nishibori, M Takata, M Sakata, K Ohoyama, K Kitazawa, H Takagi *Phys. Rev. B* **66** 134434 (2002)
65. A A Bosak, C Dubourdieu, J P Sénateur, O Yu Gorbenko, A R Kaul *J. Mater. Chem.* **12** 800 (2002)
66. I E Graboy, A A Bosak, O Yu Gorbenko, A R Kaul, C Dubourdieu, J P Sénateur, V L Svetchnikov, H W Zandbergen *Chem. Mater.* **15** 2632 (2003)
67. K R Balasubramanian, A A Bagal, O Castillo, A J Francis, P A Salvador *Ceram. Trans.* **162** 59 (2005)
68. A Posadas, J-B Yau, C H Ahn *Phys. Status Solidi B* **243** 2085 (2006)
69. K R Balasubramanian, S Havelia, P A Salvador, H Zheng, J F Mitchell *Appl. Phys. Lett.* **91** 232901 (2007)
70. K R Balasubramanian, K-C Chang, F A Mohammad, L M Porter, P A Salvador, J DiMaio, R F Davis *Thin Solid Films* **515** 1807 (2006)
71. J H Lee, P Murugavel, D Lee, T W Noh, Y Jo, M-H Jung, K H Jang, J-G Park *Appl. Phys. Lett.* **90** 012903 (2007)
72. S Nandi, A Kreyssig, J Q Yan, M D Vannette, J C Lang, L Tan, J W Kim, R Prozorov, T A Lograsso, R J McQueeney, A I Goldman *Phys. Rev. B* **78** 075118 (2008)
73. W S Choi, S J Moon, B C Jeon, J H Lee, Y S Lee *J. Korean Phys. Soc.* **55** 754 (2009)
74. D Lee, J-H Lee, P Murugavel, S Y Jang, T W Noh, Y Jo, M-H Jung, Y-D Ko, J-S Chung *Appl. Phys. Lett.* **90** 182504 (2007)
75. T Lottermoser, T Lonkai, U Amann, D Hohlwein, J Ihringer, M Fiebig *Nature (London)* **430** 541 (2004)
76. R Feyerherm, E Dudzik, A U B Wolter, S Valencia, O Prokhnenko, A Maljuk, S Landsgesell, N Aliouane, L Bouchenoire, S Brown, D N Argyriou *Phys. Rev. B* **79** 134426 (2009)
77. T Kimura, T Goto, H Shintani, K Ishizaka, T Arima, Y Tokura *Nature (London)* **426** 55 (2003)
78. M Kenzelmann, A B Harris, S Jonas, C Broholm, J Schefer, S B Kim, C L Zhang, S-W Cheong, O P Vajk, J W Lynn *Phys. Rev. Lett.* **95** 087206 (2005)
79. A A Bosak, A A Kamenev, I E Graboy, S V Antonov, O Yu Gorbenko, A R Kaul, C Dubourdieu, J P Sénateur, V L Svechnikov, H W Zandbergen, B Hollander *Thin Solid Films* **400** 149 (2001)
80. B Lorenz, Y-Q Wang, C-W Chu *Phys. Rev. B* **76** 104405 (2007)
81. V Yu Pomjakushin, M Kenzelmann, A Dlnni, A B Harris, T Nakajima, S Mitsuda, M Tachibana, L Keller, J Mesot, H Kitazawa, E Takayama-Muromachi *New J. Phys.* **11** 043019 (2009)
82. Y Mizoguchi, H Onodera, H Yamauchi, M Kagawa, Y Syono, T Hirai *Mater. Sci. Eng., A* **217** 164 (1996)
83. A A Bossak, I E Graboy, O Yu Gorbenko, A R Kaul, M S Kartavtseva, V L Svetchnikov, H W Zandbergen *Chem. Mater.* **16** 1751 (2004)
84. A R Akbashev, A S Semisalova, N S Perov, A R Kaul *Appl. Phys. Lett.* **99** 122502 (2011)
85. E Magome, C Moriyoshi, Y Kuroiwa, A Masuno, H Inoue *Jpn. J. Appl. Phys.* **49** 09ME06 (2010)
86. B B Van Aken, A Meetsma, T T M Palstra *Acta Crystallogr., Sect. C: Cryst. Struct. Commun.* **57** 230 (2001)
87. J Kim, K C Cho, Y M Koo, K P Hong, N Shin *Appl. Phys. Lett.* **95** 132901 (2009)
88. N Ikeda, K Kohn, N Myouga, E Takahashi, H Kitoh, S Takekawa *J. Phys. Soc. Jpn.* **69** 1526 (2000)
89. Y Yamada, K Kitsuda, S Nohdo, N Ikeda *Phys. Rev. B* **62** 12167 (2000)
90. A D Christianson, M D Lumsden, M Angst, Z Yamani, W Tian, R Jin, E A Payzant, S E Nagler, B C Sales, D Mandrus *Phys. Rev. Lett.* **100** 107601 (2008)
91. M H Phan, N A Frey, M Angst, J de Groot, B C Sales, D G Mandrus, H Srikanth *Solid State Commun.* **150** 341 (2010)
92. S Funahashi, J Akimitsu, K Siratori, N Kimizuka, M Tanaka, H Fujishita *J. Phys. Soc. Jpn.* **53** 2688 (1984)
93. J Iida, S Takekawa, N Kimizuka *J. Cryst. Growth* **102** 398 (1990)
94. N Kimizuka, E Takayama-Muromachi, K Siratori *Handbook on the Physics and Chemistry of Rare Earths* Vol. 13 (Eds K A Gschneidner Jr, L Eyring) (Amsterdam: Elsevier, 1990) p. 283
95. K Yoshii, N Ikeda, Y Okajima, Y Yoneda, Y Matsuo, Y Horibe, S Mori *Inorg. Chem.* **47** 6493 (2008)
96. N Kimizuka, T Mohri *J. Solid State Chem.* **60** 382 (1985)
97. J Liu, Y Wang, J Y Dai *Thin Solid Films* **518** 6909 (2010)
98. M Seki, T Konya, K Inaba, H Tabata *Appl. Phys. Express* **3** 105801 (2010)
99. J van den Brink, D I Khomskii *J. Phys.: Condens. Matter* **20** 434217 (2008)
100. A Daoud-Aladine, J Rodríguez-Carvajal, L Pinsard-Gaudart, M T Fernández-Díaz, A Revcolevschi *Phys. Rev. Lett.* **89** 097205 (2002)
101. D V Efremov, J van den Brink, D I Khomskii *Nat. Mater.* **3** 853 (2004)
102. C Jooss, L Wu, T Beetz, R F Klie, M Beleggia, M A Schofield, S Schramm, J Hoffmann, Y Zhu *Proc. Natl. Acad. Sci. USA* **104** 13597 (2007)
103. A M L Lopes, J P Araújo, V S Amaral, J G Correia, Y Tomioka, Y Tokura *Phys. Rev. Lett.* **100** 155702 (2008)
104. S Quezel-Ambrunaz, E F Bertaut, G Buisson *C. R. Acad. Sci.* **258** 3025 (1964)
105. J A Alonso, M T Casais, M J Martínez-Lope, L L Martínez, M T Fernández-Díaz *J. Phys.: Condens. Matter* **9** 8515 (1997)
106. S W Cheong, M Mostovoy *Nat. Mater.* **6** 13 (2007)
107. M J Martínez-Lope, M Retuerto, M García-Hernández, J A Alonso *J. Solid State Chem.* **182** 532 (2009)
108. A Muñoz, J A Alonso, M T Casais, M J Martínez-Lope, J L Martínez, M T Fernández-Díaz *Phys. Rev. B* **65** 144423 (2002)
109. A Muñoz, J A Alonso, M J Martínez-Lope, J L Martínez *Chem. Mater.* **16** 4087 (2004)
110. Y Chen, H Yuan, G Tian, G Zhang, S Feng *J. Solid State Chem.* **180** 1340 (2007)
111. B M Wanklyn *J. Mater. Sci.* **7** 813 (1972)
112. V A Sanina, L M Sapozhnikova, E I Golovenchits, N V Morozov *Fiz. Tv. Tela* **30** 3015 (1988) [b]
113. J A Alonso, J L García-Muñoz, M T Fernández-Díaz, M A G Aranda, M J Martínez-Lope, M T Casais *Phys. Rev. Lett.* **82** 3871 (1999)
114. G Giovannetti, S Kumar, D Khomskii, S Picozzi, J van den Brink *Phys. Rev. Lett.* **103** 156401 (2009)
115. J L García-Muñoz, J Rodríguez-Sarvajal, P Lacorre *Europhys. Lett.* **20** 241 (1992)
116. O Yu Gorbenko, M A Novojilov, I E Graboy, V Amelichev, A A Bosak, I V Nikulin, A R Kaul, B Guettler, G Wahl, N A Babushkina, L M Belova, H W Zandbergen *Int. J. Inorg. Mater.* **3** 1303 (2001)
117. G Catalan, R M Bowman, J M Gregg *J. Appl. Phys.* **87** 606 (2000)
118. M A Novojilov, O Yu Gorbenko, I E Graboy, A R Kaul, H W Zandbergen, N A Babushkina, L M Belova *Appl. Phys. Lett.* **76** 2041 (2000)
119. Y J Choi, H T Yi, S Lee, Q Huang, V Kiryukhin, S-W Cheong *Phys. Rev. Lett.* **100** 047601 (2008)
120. A Maignan, C Michel, A C Masset, C Martin, B Raveau *Eur. Phys. J. B* **15** 657 (2000)

121. R Berger *J. Less-Common Met.* **169** 33 (1991)
122. S Park, Y J Choi, C L Zhang, S-W Cheong *Phys. Rev. Lett.* **98** 057601 (2007)
123. M A Lafontaine, M Leblanc, G Ferey *Acta Crystallogr., Sect. C* **45** 1205 (1989)
124. S Masatoshi, Y Yukio, K Yoshiaki, S Kenji, N Yutaka, T Yasuko, K Yuji *Solid State Sci.* **12** 670 (2010)
125. Y Naito, K Sato, Y Yasui, Yus Kobayashi, Yos Kobayashi, M Sato *J. Phys. Soc. Jpn.* **76** 023708 (2007)
126. T Kimura, Y Sekio, H Nakamura, T Siegrist, A P Ramirez *Nat. Mater.* **7** 291 (2008)
127. W Siemons, G Koster, D H A Blank, R H Hammond, T H Geballe, M R Beasley *Phys. Rev. B* **79** 195122 (2009)
128. S Seki, T Kurumaji, S Ishiwata, H Matsui, H Murakawa, Y Tokunaga, Y Kaneko, T Hasegawa, Y Tokura *Phys. Rev. B* **82** 064424 (2010)
129. N Momozawa, Y Yamaguchi *J. Phys. Soc. Jpn.* **62** 1292 (1993)
130. T Kimura, G Lawes, A P Ramirez *Phys. Rev. Lett.* **94** 137201 (2005)
131. S Ishiwata, Y Taguchi, H Murakawa, Y Onose, Y Tokura *Science* **319** 1643 (2008)
132. S Ishiwata, D Okuyama, K Kakurai, M Nishi, Y Taguchi, Y Tokura *Phys. Rev. B* **81** 174418 (2010)
133. S H Chun, Y S Chai, Y S Oh, D Jaiswal-Nagar, S Y Haam, I Kim, B Lee, D H Nam, K-T Ko, J-H Park, J-H Chung, K H Kim *Phys. Rev. Lett.* **104** 037204 (2010)
134. S Ishiwata, Y Taguchi, Y Tokunaga, H Murakawa, Y Onose, Y Tokura *Phys. Rev. B* **79** 180408 (2009)
135. Y Takada, T Nakagawa, M Tokunaga, Y Fukuta, T Tanaka, T A Yamamoto, T Tachibana, S Kawano, Y Ishii, N Igawa *J. Appl. Phys.* **100** 043904 (2006)
136. Y Takada, T Tachibana, T Nakagawa, T A Yamamoto, T Shimada, S Kawano *J. Jpn. Soc. Powder Powder Metallurg.* **50** 618 (2003)
137. M Soda, T Ishikura, H Nakamura, Y Wakabayashi, T Kimura *Phys. Rev. Lett.* **106** 087201 (2011)
138. O P Aleshko-Ozhevskii, R A Sizov, V P Cheparin, I I Yamzin *Pis'ma Zh. Eksp. Teor. Fiz.* **7** 207 (1968) [d]
139. O P Aleshko-Ozhevskii, R A Sizov, I I Yamzin, V A Lyubimtsev *Zh. Eksp. Teor. Fiz.* **55** 820 (1968) [a]
140. Y Tokunaga, Y Kaneko, D Okuyama, S Ishiwata, T Arima, S Wakimoto, K Kakurai, Y Taguchi, Y Tokura *Phys. Rev. Lett.* **105** 257201 (2010)
141. H Weitzel *Z. Kristallogr.* **144** 238 (1976)
142. G Lautenschlager, H Weitzel, T Vogt, R Hock, A Böhm, M Bonnet, H Fuess *Phys. Rev. B* **48** 6087 (1993)
143. K Taniguchi, N Abe, T Takenobu, Y Iwasa, T Arima *Phys. Rev. Lett.* **97** 097203 (2006)
144. A H Arkenbout, T T M Palstra, T Siegrist, T Kimura *Phys. Rev. B* **74** 184431 (2006)
145. N Hollmann, Z Hu, T Willers, L Bohatý, P Becker, A Tanaka, H H Hsieh, H J Lin, C T Chen, L H Tjeng *Phys. Rev. B* **82** 184429 (2010)
146. R P Chaudhury, F Ye, J A Fernandez-Baca, Y-Q Wang, Y Y Sun, B Lorenz, H A Mook, C W Chu *Phys. Rev. B* **82** 184422 (2010)
147. F Ye, Y Ren, J A Fernandez-Baca, H A Mook, J W Lynn, R P Chaudhury, Y Q Wang, B Lorenz, C W Chu *Phys. Rev. B* **78** 193101 (2008)
148. R P Chaudhury, B Lorenz, Y Q Wang, Y Y Sun, C W Chu *New J. Phys.* **11** 033036 (2009)
149. N Rogado, G Lawes, D A Huse, A P Ramirez, R J Cava *Solid State Commun.* **124** 229 (2002)
150. G Lawes, M Kenzelmann, N Rogado, K H Kim, G A Jorge, R J Cava, A Aharony, O Entin-Wohlman, A B Harris, T Yildirim, Q Z Huang, S Park, C Broholm, A P Ramirez *Phys. Rev. Lett.* **93** 247201 (2004)
151. G Lawes, A B Harris, T Kimura, N Rogado, R J Cava, A Aharony, O Entin-Wohlman, T Yildirim, M Kenzelmann, C Broholm, A P Ramirez *Phys. Rev. Lett.* **95** 087205 (2005)
152. P Kharel, A Kumarasiri, A Dixit, N Rogado, R J Cava, G Lawes *Philos. Mag.* **89** 1923 (2009)
153. R P Chaudhury, F Yen, C R de la Cruz, B Lorenz, Y Q Wang, Y Y Sun, C W Chu *Phys. Rev. B* **75** 012407 (2007)
154. E E Sauerbrei, R Faggiani, C Calvo *Acta Crystallogr., Sect. B* **29** 2304 (1973)
155. E Morosan, J Fleitman, T Klimczuk, R J Cava *Phys. Rev. B* **76** 144403 (2007)
156. Z He, Y Ueda, M Itoh *J. Cryst. Growth* **297** 1 (2006)
157. W C Sheets, E Mugnier, A Barnabé, T J Marks, K R Poeppelmeier *Chem. Mater.* **18** 7 (2006)
158. M A Marquardt, N A Ashmore, D P Cann *Thin Solid Films* **496** 146 (2006)
159. T Kimura, J C Lashley, A P Ramirez *Phys. Rev. B* **73** 220401 (2006)
160. S Seki, Y Yamasaki, Y Shiomi, S Iguchi, Y Onose, Y Tokura *Phys. Rev. B* **75** 100403(R) (2007)
161. N Terada, S Mitsuda, K Prokes, O Suzuki, H Kitazawa, H A Katori *Phys. Rev. B* **70** 174412 (2004)
162. N Terada, T Nakajima, S Mitsuda, H Kitazawa, K Kaneko, N Metoki *Phys. Rev. B* **78** 014101 (2008)
163. E Pachoud, C Martin, B Kundys, C Simon, A Maignan *J. Solid State Chem.* **183** 344 (2010)
164. K Kimura, H Nakamura, K Ohgushi, T Kimura *Phys. Rev. B* **78** 140401 (2008)
165. S Seki, Y Onose, Y Tokura *Phys. Rev. Lett.* **101** 067204 (2008)
166. K Singh, A Maignan, C Martin, C Simon *Chem. Mater.* **21** 5007 (2009)
167. T-R Zhao, M Hasegawa, H Takei *J. Cryst. Growth* **166** 408 (1996)
168. I B Kutsenok, Candidate Thesis in Chemical Sciences, Moscow State University, Moscow, 1976
169. J E Clayton, D P Cann, N Ashmore *Thin Solid Films* **411** 140 (2002)
170. D Y Shahriari, N Erdman, U T M Haug, M C Zarzyczny, L D Marks, K R Poeppelmeier *J. Phys. Chem. Solids* **64** 1437 (2003)
171. H Hiraga, T Fukumura, A Ohtomo, T Makino, A Ohkubo, H Kimura, M Kawasaki *Appl. Phys. Lett.* **95** 032109 (2009)
172. Y Kakehi, K Satoh, T Yotsuya, S Nakao, T Yoshimura, A Ashida, N Fujimura *J. Appl. Phys.* **97** 083535 (2005)
173. J-C Lee, Y-W Heo, J-H Lee, J-J Kim *Thin Solid Films* **518** 1234 (2009)
174. Y J Choi, J Okamoto, D J Huang, K S Chao, H J Lin, C T Chen, M van Veenendaal, T A Kaplan, S-W Cheong *Phys. Rev. Lett.* **102** 067601 (2009)
175. Y Yamasaki, S Miyasaka, Y Kaneko, J P He, T Arima, Y Tokura *Phys. Rev. Lett.* **96** 207204 (2006)
176. G Giovannetti, A Stroppa, S Picozzi, D Baldomir, V Pardo, S Blanco-Canosa, F Rivadulla, S Jodlauk, D Niermann, J Rohrkamp, T Lorenz, S Streltsov, D I Khomskii, J Hemberger *Phys. Rev. B* **83** 060402 (2011)
177. M Cameron, J J Papike *Am. Mineral.* **66** 1 (1981)
178. S Jodlauk, P Becker, J A Mydosh, D I Khomskii, T Lorenz, S V Streltsov, D C Hezel, L Bohatý *J. Phys.: Condens. Matter* **19** 432201 (2007)
179. G Nénert, M Isobe, I Kim, C Ritter, C V Colin, A N Vasiliev, K H Kim, Y Ueda *Phys. Rev. B* **82** 024429 (2010)
180. M Josse, O Bidault, F Roulland, E Castel, A Simon, D Michau, R Von der Muhll, O Nguyen, M Maglione *Solid State Sci.* **11** 1118 (2009)

181. M Kenzelmann, G Lawes, A B Harris, G Gasparovic, C Broholm, A P Ramirez, G A Jorge, M Jaime, S Park, Q Huang, A Y Shapiro, L A Demianets *Phys. Rev. Lett.* **98** 267205 (2007)
182. M Pregelj, A Zorko, O Zaharko, Z Kutnjak, M Jagodič, Z Jagličić, H Berger, M de Souza, C Balz, M Lang, D Arčon *Phys. Rev. B* **82** 144438 (2010)
183. H X Yang, H F Tian, Y J Song, Y B Qin, Y G Zhao, C Ma, J Q Li *Phys. Rev. Lett.* **106** 016406 (2011)
184. H Murakawa, Y Onose, S Miyahara, N Furukawa, Y Tokura *Phys. Rev. Lett.* **105** 137202 (2010)
185. J P Remeika *J. Appl. Phys.* **31** S263 (1960)
186. A Daoud-Aladine, B Kundys, C Martin, P G Radaelli, P J Brown, C Simon, L C Chapon *Phys. Rev. B* **80** 220402 (2009)
187. R E Newnham, J J Kramer, W A Schulze, L E Cross *J. Appl. Phys.* **49** 6088 (1978)
188. J R Sahu, C R Serrao, N Ray, U V Waghmare, C N R Rao *J. Mater. Chem.* **17** 42 (2007)
189. A M Kadomtseva, Yu F Popov, G P Vorob'ev, A P Pyatakov, S S Krotov, K I Kamilov, V Yu Ivanov, A A Mukhin, A K Zvezdin, A M Kuz'menko, L N Bezmaternykh, I A Gudim, V L Temerov *Fiz. Nizk. Temp.* **36** 640 (2010) [e]
190. J F Scott, R Blinc *J. Phys.: Condens. Matter* **23** 113202 (2011)
191. E T Keve, S C Abrahams, J M Bernstein *J. Chem. Phys.* **51** 4928 (1969)
192. M Eibschmtz, H J Guggenheim, S H Wemple, I Camlibel, M DiDomenico Jr *Phys. Lett. A* **29** 409 (1969)
193. J Ravez *J. Phys. III* **7** 1129 (1997)
194. D E Cox, M Eibschütz, H Guggenhe, L Holmes *J. Appl. Phys.* **41** 943 (1970)
195. M Eibschut, H J Guggenheim *Solid State Commun.* **6** 737 (1968)
196. R Blinc, G Tavčar, B Žemva, D Hanžel, P Cevc, C Filipič, A Levstik, Z Jagličić, Z Trontelj, N Dalal, V Ramachandran, S Nellutla, J F Scott *J. Appl. Phys.* **103** 074114 (2008)
197. J Ravez, S C Abrahams, R de Pape *J. Appl. Phys.* **65** 3987 (1989)
198. J Ravez, S Abrahams, A Simon, Y Calage, R de Pape *Ferroelectrics* **108** 91 (1990)
199. S W Kim, H Y Chang, P S Halasyamani *J. Am. Chem. Soc.* **132** 17684 (2010)
200. B Kundys, A Lappas, M Viret, V Kapustianyk, V Rudyk, S Semak, C Simon, I Bakaimi *Phys. Rev. B* **81** 224434 (2010)
201. S Horiuchi, Y Tokura *Nat. Mater.* **7** 357 (2008)
202. J Ma, J Hu, Z Li, C-W Nan *Adv. Mater.* **23** 1062 (2011)
203. C-W Nan, M I Bichurin, S Dong, D Viehland, G Srinivasan *J. Appl. Phys.* **103** 031101 (2008)
204. G Srinivasan *Annu. Rev. Mater. Res.* **40** 153 (2010)
205. C A F Vaz, J Hoffman, C H Anh, R Ramesh *Adv. Mater.* **22** 2900 (2010)
206. L P Curecheriu, M T Buscaglia, V Buscaglia, L Mitoseriu, P Postolache, A Ianculescu, P Nanni *J. Appl. Phys.* **107** 104106 (2010)
207. M A Zurbuchen, T Wu, S Saha, J Mitchell, S K Streiffer *Appl. Phys. Lett.* **87** 232908 (2005)
208. M I Bichurin, V M Petrov, G Srinivasan *Phys. Rev. B* **68** 054402 (2003)
209. H Zheng, J Wang, S E Lofland, Z Ma, L Mohaddes-Ardabili, T Zhao, L Salamanca-Riba, S R Shinde, S B Ogale, F Bai, D Viehland, Y Jia, D G Schlom, M Wuttig, A Roytburd, R Ramesh *Science* **303** 661 (2004)
210. J Boomgaard, D R Terrell, R A J Born, H F J I Giller *J. Mater. Sci.* **9** 1705 (1974)
211. A R Akbashev, O Yu Gorbenko, A R Kaul *Al'tern. Energ. Ekol.* (1) 55 (2008) [f]
212. I Sosnowska, R Przenioslo, P Fischer, V A Murashov *J. Magn. Magn. Mater.* **160** 384 (1996)
213. J Wang, J B Neaton, H Zheng, V Nagarajan, S B Ogale, B Liu, D Viehland, V Vaithyanathan, D G Schlom, U V Waghmare, N A Spaldin, K M Rabe, M Wuttig, R Ramesh *Science* **299** 1719 (2003)
214. M Fiebig, D Fröhlich, K Kohn, S Leute, T Lottermoser, V V Pavlov, R V Pisarev *Phys. Rev. Lett.* **84** 5620 (2000)
215. A M Kadomtseva, S S Krotov, Yu F Popov, G P Vorob'ev *Fiz. Nizk. Temper.* **32** 933 (2006) [e]
216. Y Noda, H Kimura, M Fukunaga, S Kobayashi, I Kagomiya, K Kohn *J. Phys.: Condens. Matter* **20** 434206 (2008)
217. S D Kaushik, S Rayaprol, J Saha, N Mohapatra, V Siruguri, P D Babu, S Patnaik, E V Sampathkumaran *J. Appl. Phys.* **108** 084106 (2010)
218. T Masuda, A Zheludev, A Bush, M Markina, A Vasiliev *Phys. Rev. Lett.* **92** 177201 (2004)

[a] — *J. Exp. Theor. Phys. (Engl. Transl.)*
[b] — *Phys. Solid State (Engl. Transl.)*
[c] — *Physics-Uspekhi (Engl. Transl.)*
[d] — *J. Exp. Theor. Phys. Lett. (Engl. Transl.)*
[e] — *Low Temp. Phys. (Engl. Transl.)*
[f] — *Int. Sci. J. Altern. Energ. Ecol. (Engl. Transl.)*